Braiding, Majorana Fermions, Fibonacci Particles and Topological Quantum Computing

Louis H. Kauffman
Department of Mathematics, Statistics and Computer Science
University of Illinois at Chicago
851 South Morgan Street
Chicago, IL, 60607-7045
and
Department of Mechanics and Mathematics
Novosibirsk State University
Novosibirsk, Russia
<kauffman@uic.edu>
and
Samuel J. Lomonaco.
Department of Computer Science and Electrical Engineering
University of Maryland Baltimore County
1000 Hilltop Circle
Baltimore, MD 21250
< lomonaco@umbc.edu>

Abstract. This paper is an introduction to relationships between topology, quantum computing and the properties of Fermions. In particular we study the remarkable unitary braid group representations associated with Majorana Fermions.

Keywords. braiding, Fermions, majorana Fermions, quantum process, quantum computing.

1 Introduction

In this paper we study a Clifford algebra generalization of the quaternions and its relationship with braid group representations related to Majorana Fermion operators. Majorana Fermion operators

a and b are defined, so that the creation and annihilation operators $\psi^\dagger$ and ψ for a single standard Fermion satisfy the well known algebraic rules:

$$(\psi^\dagger)^2 = \psi^2 = 0,$$

$$\psi\psi^\dagger + \psi^\dagger\psi = 1.$$

Remarkably, these equations are satisfied if we take

$$\psi = a + ib,$$

$$\psi^\dagger = a - ib$$

where the Majorana operators a, b satisfy

$$a^\dagger = a, b^\dagger = b,$$

$$a^2 = b^2 = 1, ab + ba = 0.$$

In certain situations, it has been conjectured and partially verified by experiments that electrons (in low temperature nano-wires) may behave as though each electron were physically a pair of Majorana particles described by these Majorana operators. In this case the mathematics of the braid group representations that we study may have physical reality.

Particles corresponding to the Clifford algebra generated by a and b described in the last paragraph are called Majorana particles because they satisfy $a^\dagger = a$ and $b^\dagger = b$ indicating that they are their own anti-particles. Majorana [72] analyzed real solutions to the Dirac equation [17, 41] and conjectured the existence of such particles that would be their own anti-particle. It has been conjectured that the neutrino is such a particle. Only more recently [26, 65] has it been suggested that electrons may be composed of pairs of Majorana particles. It is common to speak of Majorana particles when referring to particles that satisfy the interaction rules for the original Majorana particles. These interaction rules are, for a given particle P, that P can interact with another identical P to produce a single P or to produce an annihilation. For this, we write

$$PP = P + 1$$

where the right hand side is to be read as a superposition of the possibilities P and 1 where 1 stands for the state of annihilation, the absence of the particle P. We refer to this equation as *the fusion rules for a Majorana Fermion*. Thus there are two algebraic descriptions for Majorana Fermions – the fusion rules and the associated Clifford algebra. One may use both the Clifford algebra and the fusion rules in a single physical situation. However, for studying braiding, it turns out that the Clifford algebra leads to braiding and so does the fusion algebra in the so-called Fibonacci model (while the Fibonacci model is not directly related to the Clifford algebra). Thus we shall discuss two forms of braiding. We shall see mathematical commonality between them. It is a matter of speculation whether both forms of braiding could be present in a single physical

system.

Braiding operators associated with Majorana operators can be very simply described. Let $\{c_1, c_2, \cdots, c_n\}$ denote a collection of Majorana operators such that $(c_k)^2 = 1$ for $k = 1, \cdots, n$ and $c_i c_j + c_j c_i = 0$ when $i \neq j$. Take the indices $\{1, 2, ..., n\}$ as a set of residuces modulo n so that $n + 1 = 1$. Define operators

$$\tau_k = (1 + c_{k+1} c_k)/\sqrt{2}$$

for $k = 1, \cdots n$ where it is understood that $c_{n+1} = c_1$ since $n + 1 = 1$ modulo n. Then one can verify that

$$\tau_i \tau_j = \tau_j \tau_i$$

when $|i - j| \geq 2$ and that

$$\tau_i \tau_{i+1} \tau_i = \tau_{i+1} \tau_i \tau_{i+1}$$

for all $i = 1, \cdots n$. Thus

$$\{\tau_1, \cdots, \tau_{n-1}\}$$

describes a representation of the n-strand Artin Braid Group B_n. As we shall see in Section 3, this representation has very interesting properties and it leads to unitary representations of the braid group that can support partial topological computing. What is missing to support full topological quantum computing in this representation is a sufficient structure of $U(2)$ transformations. These must be supplied along with the braiding operators. It remains to be seen if the braiding of Majorana operator constituents of electrons can be measured and if the physical world will yield this form of partial topological computing.

The Fibonacci model for topological quantum computing is based on the fusion rules for a Majorana Fermion as we have described them above. The particles described as Fibonacci anyons correspond, in theory, to collectivities of electrons, as in the quantum Hall effect. Fusion rules for such quasiparticles were conjectured in the work of Moore and Read [75] as part of a larger conjecture that links the fractional quantum Hall effect with Chern-Simons Theory and with the braiding representations associated via conformal field theory, with Chern-Simons Theory. These braiding representations have been described in the context of combinatorial topology via Temperley-Lieb recoupling theory [34, 38] and it is this basis for the braiding of Fibonacci particles that we shall describe here. In this form the Chern-Simons theory is not directly mentioned in constructing the braiding and our work is based on the bracket model of the Jones polynomial. The fusion rule $PP = P + 1$ is an expression of the possibilities in recoupling a Jones-Wenzl projector, as we shall see in Section 9. Thus our Fibonacci particles can be regarded as Majorana Fermions in the sense of Majorana, in that they are their own anti-particles, but we do not use the creation/annihilation algebra for them, nor do we directly associate the braiding representations associated with the Clifford algebra of Majorana operators. For this reason, we refrain from calling Fibonacci particles by the term Majorana and reserve the term Majorana particle to one that is associated with the Clifford algebra as described above. Nevertheless, it should be pointed out

that recent research analyzes edge effects in the quasi-particles of the quantum Hall system by looking at Majorana modes in the electrons that compose the quasi-particles [3].

The purpose of this paper is to discuss these braiding representations, important for relationships among physics, quantum information and topology. A new result in this paper is the Clifford Braiding Theorem of Section 3. This theorem shows that the Majorana operators give rise to a particularly robust representation of the braid group that is then further represented to find the phases of the Fermions under their exchanges in a plane space. This more robust representation in our braiding theorem will be the subject of further work. The latter part of the paper investigates the representations of the braid group that are called the Fibonacci Model for interacting anyons in a plane physical space. Here the anyons are described via their fusion algebra and they represent collectivities of electrons. In modeling the quantum Hall effect [85, 19, 10, 11], the braiding of quasi-particles (collective excitations) leads to non-trival representations of the Artin braid group. Such particles are called *Anyons*. The braiding in these models is related to topological quantum field theory.

Topological quantum computing. For the sake of background, here is a very condensed presentation of how unitary representations of the braid group are constructed via topological quantum field theoretic methods, leading to the Fibonacci model and its generalizations. One has a mathematical particle with label P that can interact with itself to produce either itself labeled P or itself with the null label $*$. We shall denote the interaction of two particles P and Q by the expression PQ, but it is understood that the "value" of PQ is the result of the interaction, and this may partake of a number of possibilities. Thus for our particle P, we have that PP may be equal to P or to $*$ in a given situation. When $*$ interacts with P the result is always P. When $*$ interacts with $*$ the result is always $*$. One considers process spaces where a row of particles labeled P can successively interact, *subject to the restriction that the end result is* P. For example the space $V[(ab)c]$ denotes the space whose basis consists in the possible interaction sequences of three particles labeled P. The particles are placed in the positions a, b, c. Thus we begin with $(PP)P$. In a typical sequence of interactions, the first two P's interact to produce a $*$, and the $*$ interacts with P to produce P.

$$(PP)P \longrightarrow (*)P \longrightarrow P.$$

In another possibility, the first two P's interact to produce a P, and the P interacts with P to produce P.

$$(PP)P \longrightarrow (P)P \longrightarrow P.$$

It follows from this analysis that the space of linear combinations of processes $V[(ab)c]$ is two dimensional. The two processes we have just described can be taken to be the qubit basis for this space. One obtains a representation of the three strand Artin braid group on $V[(ab)c]$ by assigning appropriate phase changes to each of the generating processes. One can think of these phases as corresponding to the interchange of the particles labeled a and b in the association $(ab)c$. The other operator for this representation corresponds to the interchange of b and c. This interchange is accomplished by a *unitary change of basis mapping*

$$F : V[(ab)c] \longrightarrow V[a(bc)].$$

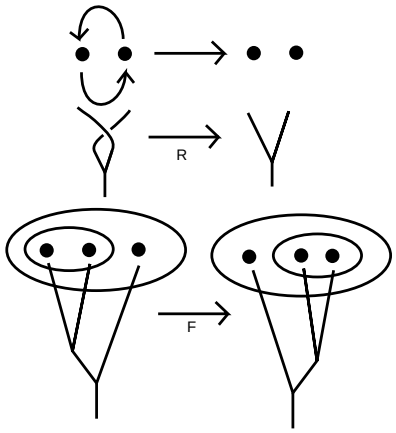

Figure 1: **Braiding Anyons**

If

$$A : V[(ab)c] \longrightarrow V[(ba)c]$$

is the first braiding operator (corresponding to an interchange of the first two particles in the association) then the second operator

$$B : V[(ab)c] \longrightarrow V[(ac)b]$$

is accomplished via the formula $B = F^{-1}RF$ where the R in this formula acts in the second vector space $V[a(bc)]$ to apply the phases for the interchange of b and c. These issues are illustrated in Figure 1, where the parenthesization of the particles is indicated by circles and by also by trees. The trees can be taken to indicate patterns of particle interaction, where two particles interact at the branch of a binary tree to produce the particle product at the root.

In this scheme, vector spaces corresponding to associated strings of particle interactions are interrelated by *recoupling transformations* that generalize the mapping F indicated above. A full representation of the Artin braid group on each space is defined in terms of the local interchange phase gates and the recoupling transformations. These gates and transformations have to satisfy a number of identities in order to produce a well-defined representation of the braid group. These identities were discovered originally in relation to topological quantum field theory. In our approach the structure of phase gates and recoupling transformations arise naturally from the structure of the bracket model for the Jones polynomial. Thus we obtain a knot-theoretic basis for topological quantum computing.

The remarkable fact about the Fibonacci model is that it is truly universal for quantum computing and so, mathematically, is a basis for topological quantum computing. At the level of three braid strands the unitary transformations of the Fibonacci model generate a dense set of elements

of $SU(2)$ and the same applies with more braid strands to $SU(N)$ where N is a Fibonacci number. Enough unitary transformations are produced to support all quantum computing within these coherent representations of the Artin braid group. True topological quantum computing would be obtained if the phases in the fractional quantum Hall effect could be correspondingly measured.

It is hoped that the mathematics we explain here will form a bridge between theoretical models of anyons and their applications to quantum computing. We have summarized the recoupling approach in order to contrast it with the way that braiding of Majorana Fermions occurs in the present paper via natural representations of Clifford algebras and also with the representations of the quaternions as $SU(2)$ to the Artin braid group. The recoupling theory is motivated by a hypothesis that one could observe the Fibonacci particles by watching their interactions and fusions. It is possible that this is a correct hypothesis for the vortices of the quantum Hall effect. It is less likely to be the right framework for electrons in one-dimensional nano-wires. Nevertheless, these two modes of creating braid group representations intersect at the place where there are only three Majorana operators, generating a copy of the quaternions. It is possible that by handling Majorana Fermions in triples in this way, one can work with the very rich braid group representations that are associated with the quaternions. We make the juxtaposition in this paper and intend further study.

The paper is organized as follows. There are 13 sections in this paper including the introduction. Section 2 is a discussion of braids and the Artin braid group. Section 3 discusses Majorana Fermions from the point of view of their quantum field theoretic annihilation and creation algebra and shows how the operator algebras for standard Fermions arise from the Clifford algebras associated with Majorana Fermions. We then show how fundamental braid group representations arise from these Clifford algebras. Section 4 discusses how appropriate unitary braiding operators can create universal gates for topological or partially topological quantum computing. Section 5 discusses the general case of $SU(2)$ representations of the Artin braid group. This section is central to the paper as a whole. We see that the braid group representations for triples of Majorana Fermions fit into this mold and that the key representation of the three strand braid group that is generalized to the Fibonacci model also occurs here. Section 6 introduces the Kauffman bracket model of the Jones polynomial and shows how to construct a quantum algorithm for it that supports its calculation for three-strand braids. This will be generalized later in the paper. Section 7 discusses the basics of quantum topology, elements of cobordism, Temperley Lieb algebra and the basics of Topological Quantum Field Theory (TQFT). Then Section 8 discusses braiding and TQFT. Section 9 introduces spin networks and the related TQFT formalism. Sections 10 and 11 show how to construct the Fibonacci model using these tools. It is here that properties of the Jones-Wenzl projectors allow the modeling of specific fusion algebras.

The next section of the paper applies the unitary braiding of the Fibonacci model to show how to formulate the topological computation of knot invariants and three-manifold invariants. Section 12 applies the (generalized) Fibonacci Model to the quantum computation of colored Jones polynomials and the Wittten-Reshetikhin-Turaev invariant of three-manifolds. Section 13

is a reconstruction of the Fibonacci model without using the recoupling theory directly, but using its underpinning, the Temperley-Lieb algebra.

Remark. The reader, particularly a physicist reader, of this paper may find that it appears sketchy since we have not done any heavy calculations. Our intent is to give a clear conceptual account of the mathematics involved in the constructions in the paper. The mathematics is fully rigorous. We have emphasized abstract arguments in an expository context. Thus we request that the reader, finding the atmosphere somewhat rarefied, to please reread the text and to work at supplying examples of his/her own that ground the work in his own ideas and understandings. We will be happy if this paper becomes a useful source of discussion about topological quantum computing and its possibilities in the physical and mathematical worlds.

Remark. Much of this paper is based upon our joint work in the papers and books [42, 46, 43, 47, 48, 49, 50, 51, 52, 53, 54, 55, 56, 58, 60, 61, 13, 38, 34, 67, 68, 69]. We have woven this work into the present paper in a form that is coupled with recent and previous work on relations with logic and with Majorana Fermions.

Acknowledgement. Kauffman's work was supported by the Laboratory of Topology and Dynamics, Novosibirsk State University (contract no. 14.Y26.31.0025 with the Ministry of Education and Science of the Russian Federation). Lomonaco's work was supported by NASA grant number NNH16ZDA001N-AIST16-0091.

2 Braids

A *braid* is an embedding of a collection of strands that have their ends in two rows of points that are set one above the other with respect to a choice of vertical. The strands are not individually knotted and they are disjoint from one another. See Figure 2, and Figure 3 for illustrations of braids and moves on braids. Braids can be multiplied by attaching the bottom row of one braid to the top row of the other braid. Taken up to ambient isotopy, fixing the endpoints, the braids form a group under this notion of multiplication. In Figure 2 we illustrate the form of the basic generators of the braid group, and the form of the relations among these generators. Figure 3 illustrates how to close a braid by attaching the top strands to the bottom strands by a collection of parallel arcs. A key theorem of Alexander states that *every knot or link can be represented as a closed braid.* The Markov Theorem [9] gives an equivalence relation on braids such that *two braids are Markov equivalent if and only if their braid closures are ambient isotopic knots or links.* Thus the theory of braids is critical to the theory of knots and links. Figure 3 illustrates the famous Borommean Rings as the closure of a braid. The Borommean Rings are a link of three unknotted loops such that any two of the loops are unlinked.

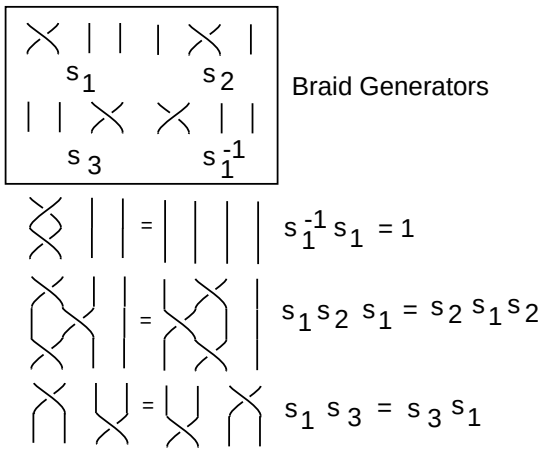

Figure 2: **Braid Generators**

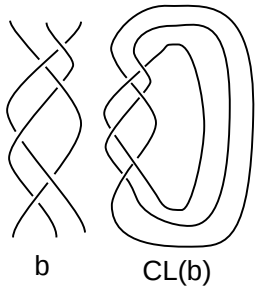

Figure 3: **Borromean Rings as a Braid Closure**

Let B_n denote the Artin braid group on n strands. We recall here that B_n is generated by elementary braids $\{s_1, \cdots, s_{n-1}\}$ with relations

1. $s_i s_j = s_j s_i$ for $|i-j| > 1$,

2. $s_i s_{i+1} s_i = s_{i+1} s_i s_{i+1}$ for $i = 1, \cdots n-2$.

See Figure 2 for an illustration of the elementary braids and their relations. Note that the braid group has a diagrammatic topological interpretation, where a braid is an intertwining of strands that lead from one set of n points to another set of n points. The braid generators s_i are represented by diagrams where the i-th and $(i+1)$-th strands wind around one another by a single half-twist (the sense of this turn is shown in Figure 2) and all other strands drop straight to the bottom. Braids are diagrammed vertically as in Figure 2, and the products are taken in order from top to bottom. The product of two braid diagrams is accomplished by adjoining the top strands of one braid to the bottom strands of the other braid.

In Figure 2 we have restricted the illustration to the four-stranded braid group B_4. In that figure the three braid generators of B_4 are shown, and then the inverse of the first generator is drawn. Following this, one sees the identities $s_1 s_1^{-1} = 1$ (where the identity element in B_4 consists in four vertical strands), $s_1 s_2 s_1 = s_2 s_1 s_2$, and finally $s_1 s_3 = s_3 s_1$.

Braids are a key structure in mathematics. It is not just that they are a collection of groups with a vivid topological interpretation. From the algebraic point of view the braid groups B_n are important extensions of the symmetric groups S_n. Recall that the symmetric group S_n of all permutations of n distinct objects has presentation as shown below.

1. $s_i^2 = 1$ for $i = 1, \cdots n-1$,

2. $s_i s_j = s_j s_i$ for $|i-j| > 1$,

3. $s_i s_{i+1} s_i = s_{i+1} s_i s_{i+1}$ for $i = 1, \cdots n-2$.

Thus S_n is obtained from B_n by setting the square of each braiding generator equal to one. We have short exact sequence

$$1 \longrightarrow P_n \longrightarrow B_n \longrightarrow S_n \longrightarrow 1$$

exhibiting the Artin braid group as an extension of the symmetric group. The kernel of the surjection of B_n to S_n is P_n, the *pure braid group on n strands*.

In the next sections we shall show how unitary representations of the Artin braid group, rich enough to provide a dense set of transformations in the unitary groups, arise in relation to Fermions, Majorana Fermions and Fibonacci particles and their generalizations. Braid groups are *in principle* fundamental to quantum computation and quantum information theory. More information about braids will appear throughout the rest of the paper. The purpose of this short section has been to give an orientation and basic definitions for braiding.

3 Fermions, Majorana Fermions and Braiding

Fermion Algebra. Recall Fermion algebra. One has Fermion annihilation operators ψ and their conjugate creation operators $\psi^\dagger$. One has $\psi^2 = 0 = (\psi^\dagger)^2$. There is a fundamental commutation relation

$$\psi\psi^\dagger + \psi^\dagger\psi = 1.$$

If you have more than one of them say ψ and ϕ, then they anti-commute:

$$\psi\phi = -\phi\psi.$$

The Majorana Fermions c satisfy $c^\dagger = c$ so that they are their own anti-particles. There is a lot of interest in these as quasi-particles and they are related to braiding and to topological quantum computing. A group of researchers [63, 7] have found quasiparticle Majorana Fermions in edge effects in nano-wires. (A line of Fermions could have a Majorana Fermion happen non-locally from one end of the line to the other.) The Fibonacci model that we discuss is also based on Majorana particles, possibly related to collective electronic excitations. If P is a Majorana Fermion particle, then P can interact with itself to either produce itself or to annihilate itself. This is the simple "fusion algebra" for this particle. One can write $P^2 = P + 1$ to denote the two possible self-interactions the particle P. The patterns of interaction and braiding of such a particle P give rise to the Fibonacci model.

Majorana Operators make Fermion Operators. Majoranas [72] are related to standard Fermions as follows: The algebra for Majoranas is $x = x^\dagger$ and $xy = -yx$ if x and y are distinct Majorana Fermions with $x^2 = 1$ and $y^2 = 1$. Thus the operator algebra for a collection of Majorana particles is a Clifford algebra. One can make a standard Fermion from two Majoranas via

$$\psi = (x + iy)/2,$$

$$\psi^\dagger = (x - iy)/2.$$

Note, for example, that

$$\psi^2 = (x + iy)(x + iy)/4 = x^2 - y^2 + i(xy + yx) = 0 + i0 = 0.$$

Similarly one can mathematically make two Majoranas from any single Fermion via

$$x = (\psi + \psi^\dagger)/2$$

$$y = (\psi + \psi^\dagger)/(2i).$$

This simple relationship between the Fermion creation and annihilation algebra and an underlying Clifford algebra has long been a subject of speculation in physics. Only recently have experiments shown (indirect) evidence [63] for Majorana Fermions underlying the electron.

Braiding. Given a set of Majorana operators

$$\{c_1, c_2, c_3, \cdots, c_n\},$$

then there are natural braiding operators [26, 65] that act on the vector space with these c_k as the basis. First, we define operators by the algebra elements

$$\tau_k = (1 + c_{k+1}c_k)/\sqrt{2},$$

$$\tau_k^{-1} = (1 - c_{k+1}c_k)/\sqrt{2}$$

for $k = 1, \cdots, n$ where we work with the set $\{1, 2, \cdots, n-1, n\}$ as the set of residues modulo n so that $n + 1$ denotes 1. The operators τ_k satisfy the braiding relations as we will show below. Ivanov [26] studies a simpler representation of the braid group where the braiding operators T_k acting on the vector space with basis $\{c_1, c_2, \cdots, c_n\}$ are defined as follows.

$$T_k : Span\{c_1, c_2, \cdots, , c_n\} \longrightarrow Span\{c_1, c_2, \cdots, , c_n\}$$

via

$$T_k(x) = \tau_k x \tau_k^{-1}.$$

The braiding is simply:

$$T_k(c_k) = c_{k+1},$$

$$T_k(c_{k+1}) = -c_k,$$

and T_k is the identity otherwise. This gives a very nice unitary representaton of the Artin braid group and it deserves better understanding.

That there is much more to this braiding is indicated by the following result.

Clifford Braiding Theorem. Let C be the Clifford algebra over the real numbers generated by linearly independent elements $\{c_1, c_2, \cdots c_n\}$ with $c_k^2 = 1$ for all k and $c_k c_l = -c_l c_k$ for $k \neq l$. Then the algebra elements $\tau_k = (1 + c_{k+1}c_k)/\sqrt{2}$, form a representation of the (circular) Artin braid group. That is, we have $\{\tau_1, \tau_2, \cdots \tau_{n-1}, \tau_n\}$ where $\tau_k = (1 + c_{k+1}c_k)/\sqrt{2}$ for $1 \leq k < n$ and $\tau_n = (1 + c_1 c_n)/\sqrt{2}$, and $\tau_k \tau_{k+1} \tau_k = \tau_{k+1} \tau_k \tau_{k+1}$ for all k and $\tau_i \tau_j = \tau_j \tau_i$ when $|i - j| \geq 2$. Note that each braiding generator τ_k has order 8. Note also that we can formally write $\tau_k = exp(c_{k+1}c_k \pi/4)$.

Proof. Let $a_k = c_{k+1}c_k$. Examine the following calculation:

$$\tau_k \tau_{k+1} \tau_k = (\frac{1}{2\sqrt{2}})(1 + a_{k+1})(1 + a_k)(1 + a_{k+1})$$

$$= (\frac{1}{2\sqrt{2}})(1 + a_k + a_{k+1} + a_{k+1}a_k)(1 + a_{k+1})$$

$$= (\frac{1}{2\sqrt{2}})(1 + a_k + a_{k+1} + a_{k+1}a_k + a_{k+1} + a_k a_{k+1} + a_{k+1}a_{k+1} + a_{k+1}a_k a_{k+1})$$

$$= (\frac{1}{2\sqrt{2}})(1 + a_k + a_{k+1} + c_{k+2}c_k + a_{k+1} + c_k c_{k+2} - 1 - c_k c_{k+1})$$

$$= (\frac{1}{2\sqrt{2}})(a_k + a_{k+1} + a_{k+1} + c_{k+1}c_k)$$

$$= (\frac{1}{2\sqrt{2}})(2a_k + 2a_{k+1})$$

$$= (\frac{1}{\sqrt{2}})(a_k + a_{k+1}).$$

Since the end result is symmetric under the interchange of k and $k+1$, we conclude that

$$\tau_k \tau_{k+1} \tau_k = \tau_{k+1} \tau_k \tau_{k+1}.$$

Note that this braiding relation works circularly if we define $\tau_n = (1 + c_1 c_n)/\sqrt{2}$. It is easy to see that $\tau_i \tau_j = \tau_j \tau_i$ when $|i - j| \geq 2$. This completes the proof. //

Undoubtedly, this representation of the (circular) Artin braid group is significant for the topological physics of Majorana Fermions. This part of the structure needs further study.

It is worth noting that a triple of Majorana Fermions say x, y, z gives rise to a representation of the quaternion group. This is a generalization of the well-known association of Pauli matrices and quaternions. We have $x^2 = y^2 = z^2 = 1$ and, when different, they anti-commute. Let $I = yx, J = zy, K = xz$. Then

$$I^2 = J^2 = K^2 = IJK = -1,$$

giving the quaternions. The operators

$$A = (1/\sqrt{2})(1 + I)$$

$$B = (1/\sqrt{2})(1 + J)$$

$$C = (1/\sqrt{2})(1 + K)$$

braid one another:

$$ABA = BAB, BCB = CBC, ACA = CAC.$$

This is a special case of the braid group representation described above for an arbitrary list of Majorana Fermions. These braiding operators are entangling and so can be used for universal quantum computation, but they give only partial topological quantum computation due to the interaction with single qubit operators not generated by them.

Here is the derivation of the braiding relation in the quaternion case.

$$ABA = (1/2\sqrt{2})(1+I)(1+J)(1+I)$$

$$= (1/2\sqrt{2})(1+I+J+IJ)(1+I)$$

$$= (1/2\sqrt{2})(1+I+J+IJ+I+I^2+JI+IJI)$$

$$= (1/2\sqrt{2})(1+I+J+IJ+I-1-IJ+J)$$

$$= (1/\sqrt{2})(I+J).$$

The same form of computation yields $BAB = (1/\sqrt{2})(J+I)$. And so

$$ABA = BAB.$$

and so a natural braid group representation arises from the Majorana Fermions.

These braiding operators can be seen to act on the vector space over the complex numbers that is spanned by the Majorana Fermion operators x, y, z. To see how this works, consider

$$\tau = \frac{1+yx}{\sqrt{2}},$$

$$T(p) = \tau p \tau^{-1} = (\frac{1+yx}{\sqrt{2}})p(\frac{1-yx}{\sqrt{2}}),$$

and verify that $T(x) = y$ and $T(y) = -x$. Now view Figure 4 where we have illustrated a topological interpretation for the braiding of two Fermions. In the topological interpretation the two Fermions are connected by a flexible belt. On interchange, the belt becomes twisted by 2π. In the topological interpretation a twist of 2π corresponds to a phase change of -1. (For more information on this topological interpretation of 2π rotation for Fermions, see [38].) Without a further choice it is not evident which particle of the pair should receive the phase change. The topology alone tells us only the relative change of phase between the two particles. The Clifford algebra for Majorana Fermions makes a specific choice in the matter and in this way fixes the representation of the braiding.

A remarkable feature of this braiding representation of Majorana Fermions is that it applies to give a representation of the n-strand braid group B_n for any row of n Majorana Fermions. It is not restricted to the quaternion algebra. Nevertheless, we shall now examine the braiding representations of the quaternions. These representations are very rich and can be used in situations (such as Fibonacci particles) involving particles that are their own anti-particles (analogous to the Majorana Fermions underlying electrons). Such particles can occur in collectivities of electrons as in the quantum Hall effect. In such situations it is theorized that one can examine the local interaction properties of the Majorana particles and then the braidings associated to triples of them (the quaternion cases) can come into play very strongly. In the case of electrons in nano-wires,

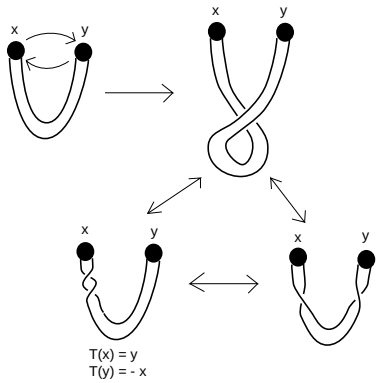

Figure 4: **Braiding Action on a Pair of Fermions**

one at the present time must make do with long range correlations between ends of the wires and forgoe such local interactions. Nevertheless, it is the purpose of this paper to juxtapose the full story about three strand braid group represenations of the quaternions in the hope that this will lead to deeper understanding of the possibilities for even the electronic Majorana Fermions.

4 Braiding Operators and Universal Quantum Gates

A key concept in the construction of quantum link invariants is the association of a Yang-Baxter [6, 88, 89] operator R to each elementary crossing in a link diagram. The operator R is a linear mapping

$$R\colon\ V \otimes V \longrightarrow V \otimes V$$

defined on the 2-fold tensor product of a vector space V, generalizing the permutation of the factors (i.e., generalizing a swap gate when V represents one qubit). Such transformations are not necessarily unitary in topological applications. It is useful to understand when they can be replaced by unitary transformations for the purpose of quantum computing. Such unitary R-matrices can be used to make unitary representations of the Artin braid group.

A solution to the Yang-Baxter equation, as described in the last paragraph is a matrix R, regarded as a mapping of a two-fold tensor product of a vector space $V \otimes V$ to itself that satisfies the equation

$$(R \otimes I)(I \otimes R)(R \otimes I) = (I \otimes R)(R \otimes I)(I \otimes R).$$

From the point of view of topology, the matrix R is regarded as representing an elementary bit of braiding represented by one string crossing over another. In Figure 5 we have illustrated the braiding identity that corresponds to the Yang-Baxter equation. Each braiding picture with its three input lines (below) and output lines (above) corresponds to a mapping of the three fold

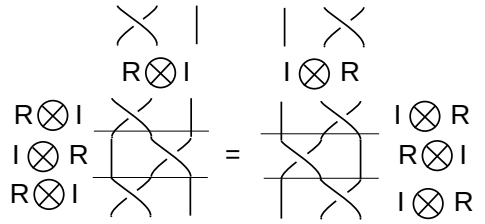

Figure 5: **The Yang-Baxter equation**

tensor product of the vector space V to itself, as required by the algebraic equation quoted above. The pattern of placement of the crossings in the diagram corresponds to the factors $R \otimes I$ and $I \otimes R$. This crucial topological move has an algebraic expression in terms of such a matrix R. We need to study solutions of the Yang-Baxter equation that are unitary. Then the R matrix can be seen *either* as a braiding matrix *or* as a quantum gate in a quantum computer.

4.1 Universal Gates

A *two-qubit gate* G is a unitary linear mapping $G : V \otimes V \longrightarrow V \otimes V$ where V is a two complex dimensional vector space. We say that the gate G is *universal for quantum computation* (or just *universal*) if G together with local unitary transformations (unitary transformations from V to V) generates all unitary transformations of the complex vector space of dimension 2^n to itself. It is well-known [76] that $CNOT$ is a universal gate. (On the standard basis, $CNOT$ is the identity when the first qubit is $|0\rangle$, and it flips the second qubit, leaving the first alone, when the first qubit is $|1\rangle$.)

A gate G, as above, is said to be *entangling* if there is a vector

$$|\alpha\beta\rangle = |\alpha\rangle \otimes |\beta\rangle \in V \otimes V$$

such that $G|\alpha\beta\rangle$ is not decomposable as a tensor product of two qubits. Under these circumstances, one says that $G|\alpha\beta\rangle$ is *entangled*.

In [12], the Brylinskis give a general criterion of G to be universal. They prove that *a two-qubit gate G is universal if and only if it is entangling.*

Remark. A two-qubit pure state

$$|\phi\rangle = a|00\rangle + b|01\rangle + c|10\rangle + d|11\rangle$$

is entangled exactly when the *determinant of the state $|\phi\rangle$ is not zero.* We define the determinant of the state to be $(ad-bc)$. We have that $(ad-bc) \neq 0$ impies that the state is not a tensor product of two single qubit states. It is easy to use this fact to check when a specific gate is, or is not, entangling.

Remark. There are many gates other than $CNOT$ that can be used as universal gates in the presence of local unitary transformations. Some of these are themselves topological (unitary solutions to the Yang-Baxter equation, see [55, 6]) and themselves generate representations of the Artin braid group. Replacing $CNOT$ by a solution to the Yang-Baxter equation does not place the local unitary transformations as part of the corresponding representation of the braid group. Thus such substitutions give only a partial solution to creating topological quantum computation.

4.2 Majorana Fermions Generate Universal Braiding Gates

Recall that in Section 3 we showed how to construct braid group representations. Let $T_k : V_n \longrightarrow V_n$ defined by

$$T_k(v) = \tau_k v \tau_k^{-1}$$

be defined as in Section 3. Note that $\tau_k^{-1} = \frac{1}{\sqrt{2}}(1 - c_{k+1}c_k)$. It is then easy to verify that

$$T_k(c_k) = c_{k+1},$$

$$T_k(c_{k+1}) = -c_k$$

and that T_k is the identity otherwise.

For universality, take $n = 4$ and regard each T_k as operating on $V \otimes V$ where V is a single qubit space. Then the braiding operator T_2 satisfies the Yang-Baxter equation and is an entangling operator. So we have universal gates (in the presence of single qubit unitary operators) from Majorana Fermions. If experimental work shows that Majorana Fermions can be detected and controlled, then it is possible that quantum computers based on these topological unitary representations will be constructed. Note that the matrix form R of T_2 is

$$R = \begin{pmatrix} 1 & 0 & 0 & 0 \\ 0 & 0 & -1 & 0 \\ 0 & 1 & 0 & 0 \\ 0 & 0 & 0 & 1 \end{pmatrix}$$

Here we take the ordered basis $\{|00\rangle, |01\rangle, |10\rangle, |11\rangle\}$ for the corresponding 2-qubit space $V \otimes V$ so that

$$R|00\rangle = |00\rangle, R|01\rangle = |10\rangle,$$

$$R|10\rangle = -|01\rangle, R|11\rangle = |11\rangle.$$

It is not hard to verify that R satisfies the Yang-Baxter Equation. To see that it is entangling we take the state $|\phi\rangle = a|0\rangle + b|1\rangle$ and test R on

$$|\phi\rangle \otimes |\phi\rangle = a^2|00\rangle + ab|01\rangle + ab|10\rangle + b^2|11\rangle$$

and find that

$$R(|\phi\rangle \otimes |\phi\rangle) = a^2|00\rangle + ab|10\rangle - ab|01\rangle + b^2|11\rangle.$$

The determinant of this state is $a^2b^2 + (ab)(ab) = 2a^2b^2$. Thus when both a and b are non-zero, we have that $R(|\phi\rangle \otimes |\phi\rangle)$ is entangled. This proves that R is an entangling operator, as we have claimed. This calculation shows that a fragment of the Majorana operator braiding can be used to make a universal quantum gate, and so to produce partial topological quantum computing if realized physically.

In fact we can say more by using the braiding operators $\tau_k = \frac{1}{\sqrt{2}}(1 + c_{k+1}c_k)$, as these operators have natural matrix representations. In particular, consider the Bell-Basis Matrix B_{II} that is given as follows:

$$B_{II} = \frac{1}{\sqrt{2}} \begin{bmatrix} 1 & 0 & 0 & 1 \\ 0 & 1 & 1 & 0 \\ 0 & -1 & 1 & 0 \\ -1 & 0 & 0 & 1 \end{bmatrix} = \frac{1}{\sqrt{2}}\big(I + M\big) \quad \big(M^2 = -1\big) \tag{1}$$

where

$$M = \begin{bmatrix} 0 & 0 & 0 & 1 \\ 0 & 0 & 1 & 0 \\ 0 & -1 & 0 & 0 \\ -1 & 0 & 0 & 0 \end{bmatrix} \tag{2}$$

and we define

$$M_i = I \otimes I \otimes \cdots I \otimes M \otimes I \otimes I \otimes \cdots \otimes I$$

where there are n tensor factors in all and M occupies the i and $i+1$-st positions. Then one can verify that theses matrices satisfy the relations of an "extraspecial 2-group" [81, 74]. The relations are as follows.

$$M_iM_{i\pm1} = -M_{i\pm1}M_i, \quad M^2 = -I, \tag{3}$$

$$M_iM_j = M_jM_{i,} \quad \big|i - j\big| \geq 2. \tag{4}$$

Kauffman and Lomonaco [55] observed that B_{II} satisfies the Yang-Baxter equation and is an entangling gate. Hence $B_{II} = \frac{1}{\sqrt{2}}\big(I+M\big) \quad \big(M^2 = -1\big)$ is a universal quantum gate in the sense of this section. It is of interest to understand the possible relationships of topological entanglement (linking and knotting) and quantum entanglement. See [55, 4] for more than one point of view on this question.

Remarks. The operators M_i take the place here of the products of Majorana Fermions $c_{i+1}c_i$ in the Ivanov picture of braid group representation in the form $\tau_i = (1/\sqrt{2})(1 + c_{i+1}c_i)$. This observation gives a concrete interpretation of these braiding operators and relates them to a Hamiltonian for a physical system by an observation of Mo-Lin Ge [74]. Mo-Lin Ge shows that the observation of Ivanov [26] that $\tau_k = (1/\sqrt{2})(1 + c_{k+1}c_k) = exp(c_{k+1}c_k\pi/4)$ can be extended by defining

$$\breve{R}_k(\theta) = e^{\theta c_{k+1}c_k}.$$

Then $\breve{R}_i(\theta)$ satisfies the full Yang-Baxter equation with rapidity parameter θ. That is, we have the equation

$$\breve{R}_i(\theta_1)\breve{R}_{i+1}(\theta_2)\breve{R}_i(\theta_3) = \breve{R}_{i+1}(\theta_3)\breve{R}_i(\theta_2)\breve{R}_{i+1}(\theta_1).$$

This makes if very clear that $\breve{R}_i(\theta)$ has physical significance, and suggests examining the physical process for a temporal evolution of the unitary operator $\breve{R}_i(\theta)$.

In fact. following [74], we can construct a Kitaev chain [65, 64] based on the solution $\breve{R}_i(\theta)$ of the Yang-Baxter Equation. Let a unitary evolution be governed by $\breve{R}_k(\theta)$. When θ in the unitary operator $\breve{R}_k(\theta)$ is time-dependent, we define a state $|\psi(t)\rangle$ by $|\psi(t)\rangle = \breve{R}_k|\psi(0)\rangle$. With the Schroedinger equation $i\hbar\frac{\partial}{\partial t}|\psi(t)\rangle = \hat{H}(t)|\psi(t)\rangle$ one obtains:

$$i\hbar\frac{\partial}{\partial t}[\breve{R}_k|\psi(0)\rangle] = \hat{H}(t)\breve{R}_k|\psi(0)\rangle. \tag{5}$$

Then the Hamiltonian $\hat{H}_k(t)$ related to the unitary operator $\breve{R}_k(\theta)$ is obtained by the formula:

$$\hat{H}_i(t) = \mathrm{i}\hbar\frac{\partial\breve{R}_k}{\partial t}\breve{R}_k^{-1}. \tag{6}$$

Substituting $\breve{R}_k(\theta) = \exp(\theta c_{k+1}c_k)$ into equation (6), we have:

$$\hat{H}_k(t) = \mathrm{i}\hbar\dot{\theta}c_{k+1}c_k. \tag{7}$$

This Hamiltonian describes the interaction between k-th and $(k+1)$-th sites via the parameter $\dot{\theta}$. When $\theta = n \times \frac{\pi}{4}$, the unitary evolution corresponds to the braiding progress of two nearest Majorana Fermion sites in the system as we have described it above. Here n is an integer and signifies the time of the braiding operation. We remark that it is interesting to examine this periodicity of the appearance of the topological phase in the time evolution of this Hamiltonian. (Compare with discussion in [62].) For applications, one may consider processes that let the Hamiltonian take the the system right to one of these topological points and then this Hamiltonian cuts off. One may also think of a mode of observation that is tuned in frequency with the appearances of the topological phase. This goes beyond the work of Ivanov, who examines the representation on Majoranas obtained by conjugating by these operators. The Ivanov representation is of order two, while this representation is of order eight.

5 $SU(2)$ Representations of the Artin Braid Group

The purpose of this section is to determine all the representations of the three strand Artin braid group B_3 to the special unitary group $SU(2)$ and concomitantly to the unitary group $U(2)$. One regards the groups $SU(2)$ and $U(2)$ as acting on a single qubit, and so $U(2)$ is usually regarded as the group of local unitary transformations in a quantum information setting. If one is looking for a coherent way to represent all unitary transformations by way of braids, then $U(2)$ is the place

to start. Here we will show that there are many representations of the three-strand braid group that generate a dense subset of $SU(2)$. Thus it is a fact that local unitary transformations can be "generated by braids" in many ways.

We begin with the structure of $SU(2)$. A matrix in $SU(2)$ has the form

$$M = \begin{pmatrix} z & w \\ -\bar{w} & \bar{z} \end{pmatrix},$$

where z and w are complex numbers, and $\bar{z}$ denotes the complex conjugate of z. To be in $SU(2)$ it is required that $Det(M) = 1$ and that $M^\dagger = M^{-1}$ where Det denotes determinant, and $M^\dagger$ is the conjugate transpose of M. Thus if $z = a + bi$ and $w = c + di$ where a, b, c, d are real numbers, and $i^2 = -1$, then

$$M = \begin{pmatrix} a + bi & c + di \\ -c + di & a - bi \end{pmatrix}$$

with $a^2 + b^2 + c^2 + d^2 = 1$. It is convenient to write

$$M = a \begin{pmatrix} 1 & 0 \\ 0 & 1 \end{pmatrix} + b \begin{pmatrix} i & 0 \\ 0 & -i \end{pmatrix} + c \begin{pmatrix} 0 & 1 \\ -1 & 0 \end{pmatrix} + d \begin{pmatrix} 0 & i \\ i & 0 \end{pmatrix},$$

and to abbreviate this decomposition as

$$M = a + bI + cJ + dK$$

where

$$1 \equiv \begin{pmatrix} 1 & 0 \\ 0 & 1 \end{pmatrix}, I \equiv \begin{pmatrix} i & 0 \\ 0 & -i \end{pmatrix}, J \equiv \begin{pmatrix} 0 & 1 \\ -1 & 0 \end{pmatrix}, K \equiv \begin{pmatrix} 0 & i \\ i & 0 \end{pmatrix}$$

so that

$$I^2 = J^2 = K^2 = IJK = -1$$

and

$$IJ = K, JK = I, KI = J$$

$$JI = -K, KJ = -I, IK = -J.$$

The algebra of $1, I, J, K$ is called the *quaternions* after William Rowan Hamilton who discovered this algebra prior to the discovery of matrix algebra. Thus the unit quaternions are identified with $SU(2)$ in this way. We shall use this identification, and some facts about the quaternions to find the $SU(2)$ representations of braiding. First we recall some facts about the quaternions.

1. Note that if $q = a + bI + cJ + dK$ (as above), then $q^\dagger = a - bI - cJ - dK$ so that $qq^\dagger = a^2 + b^2 + c^2 + d^2 = 1$.

2. A general quaternion has the form $q = a + bI + cJ + dK$ where the value of $qq^\dagger = a^2 + b^2 + c^2 + d^2$, is not fixed to unity. The *length* of q is by definition $\sqrt{qq^\dagger}$.

3. A quaternion of the form $rI+sJ+tK$ for real numbers r, s, t is said to be a *pure* quaternion. We identify the set of pure quaternions with the vector space of triples (r, s, t) of real numbers R^3.

4. Thus a general quaternion has the form $q = a + bu$ where u is a pure quaternion of unit length and a and b are arbitrary real numbers. A unit quaternion (element of $SU(2)$) has the addition property that $a^2 + b^2 = 1$.

5. If u is a pure unit length quaternion, then $u^2 = -1$. Note that the set of pure unit quaternions forms the two-dimensional sphere $S^2 = \{(r, s, t)|r^2 + s^2 + t^2 = 1\}$ in R^3.

6. If u, v are pure quaternions, then

$$uv = -u \cdot v + u \times v$$

whre $u \cdot v$ is the dot product of the vectors u and v, and $u \times v$ is the vector cross product of u and v. In fact, one can take the definition of quaternion multiplication as

$$(a + bu)(c + dv) = ac + bc(u) + ad(v) + bd(-u \cdot v + u \times v),$$

and all the above properties are consequences of this definition. Note that quaternion multiplication is associative.

7. Let $g = a+bu$ be a unit length quaternion so that $u^2 = -1$ and $a = cos(\theta/2), b = sin(\theta/2)$ for a chosen angle θ. Define $\phi_g : R^3 \longrightarrow R^3$ by the equation $\phi_g(P) = gPg^\dagger$, for P any point in R^3, regarded as a pure quaternion. Then ϕ_g is an orientation preserving rotation of R^3 (hence an element of the rotation group $SO(3)$). Specifically, ϕ_g is a rotation about the axis u by the angle θ. The mapping

$$\phi : SU(2) \longrightarrow SO(3)$$

is a two-to-one surjective map from the special unitary group to the rotation group. In quaternionic form, this result was proved by Hamilton and by Rodrigues in the middle of the nineteeth century. The specific formula for $\phi_g(P)$ as shown below:

$$\phi_g(P) = gPg^{-1} = (a^2 - b^2)P + 2ab(P \times u) + 2(P \cdot u)b^2u.$$

We want a representation of the three-strand braid group in $SU(2)$. This means that we want a homomorphism $\rho : B_3 \longrightarrow SU(2)$, and hence we want elements $g = \rho(s_1)$ and $h = \rho(s_2)$ in $SU(2)$ representing the braid group generators s_1 and s_2. Since $s_1s_2s_1 = s_2s_1s_2$ is the generating relation for B_3, the only requirement on g and h is that $ghg = hgh$. We rewrite this relation as $h^{-1}gh = ghg^{-1}$, and analyze its meaning in the unit quaternions.

Suppose that $g = a + bu$ and $h = c + dv$ where u and v are unit pure quaternions so that $a^2 + b^2 = 1$ and $c^2 + d^2 = 1$. then $ghg^{-1} = c + d\phi_g(v)$ and $h^{-1}gh = a + b\phi_{h^{-1}}(u)$. Thus it follows from the braiding relation that $a = c$, $b = \pm d$, and that $\phi_g(v) = \pm\phi_{h^{-1}}(u)$. However, in the case where there is a minus sign we have $g = a + bu$ and $h = a - bv = a + b(-v)$. Thus we can now prove the following Theorem.

Theorem. Let u and v be pure unit quaternions and $g = a + bu$ and $h = c + dv$ have unit length. Then (without loss of generality), the braid relation $ghg = hgh$ is true if and only if $h = a + bv$, and $\phi_g(v) = \phi_{h^{-1}}(u)$. Furthermore, given that $g = a + bu$ and $h = a + bv$, the condition $\phi_g(v) = \phi_{h^{-1}}(u)$ is satisfied if and only if $u \cdot v = \frac{a^2-b^2}{2b^2}$ when $u \neq v$. If $u = v$ then $g = h$ and the braid relation is trivially satisfied.

Proof. We have proved the first sentence of the Theorem in the discussion prior to its statement. Therefore assume that $g = a + bu, h = a + bv$, and $\phi_g(v) = \phi_{h^{-1}}(u)$. We have already stated the formula for $\phi_g(v)$ in the discussion about quaternions:

$$\phi_g(v) = gvg^{-1} = (a^2 - b^2)v + 2ab(v \times u) + 2(v \cdot u)b^2u.$$

By the same token, we have

$$\begin{aligned}\phi_{h^{-1}}(u) = h^{-1}uh &= (a^2 - b^2)u + 2ab(u \times -v) + 2(u \cdot (-v))b^2(-v) \\ &= (a^2 - b^2)u + 2ab(v \times u) + 2(v \cdot u)b^2(v).\end{aligned}$$

Hence we require that

$$(a^2 - b^2)v + 2(v \cdot u)b^2u = (a^2 - b^2)u + 2(v \cdot u)b^2(v).$$

This equation is equivalent to

$$2(u \cdot v)b^2(u - v) = (a^2 - b^2)(u - v).$$

If $u \neq v$, then this implies that

$$u \cdot v = \frac{a^2 - b^2}{2b^2}.$$

This completes the proof of the Theorem. //

The Majorana Fermion Example. Note the case of the theorem where

$$g = a + bu, h = a + bv.$$

Suppose that $u \cdot v = 0$. Then the theorem tells us that we need $a^2 - b^2 = 0$ and since $a^2 + b^2 = 1$, we conclude that $a = 1/\sqrt{2}$ and b likewise. For definiteness, then we have for the braiding generators (since I, J and K are mutually orthogonal) the three operators

$$A = \frac{1}{\sqrt{2}}(1 + I),$$

$$B = \frac{1}{\sqrt{2}}(1 + J),$$

$$C = \frac{1}{\sqrt{2}}(1 + K).$$

Each pair satisfies the braiding relation so that $ABA = BAB, BCB = CBC, ACA = CAC$. We have already met this braiding triplet in our discussion of the construction of braiding operators from Majorana Fermions in Section 3. This shows (again) how close Hamilton's quaternions are to topology and how braiding is fundamental to the structure of Fermionic physics.

The Fibonacci Example. Let

$$g = e^{I\theta} = a + bI$$

where $a = cos(\theta)$ and $b = sin(\theta)$. Let

$$h = a + b[(c^2 - s^2)I + 2csK]$$

where $c^2 + s^2 = 1$ and $c^2 - s^2 = \frac{a^2-b^2}{2b^2}$. Then we can rewrite g and h in matrix form as the matrices G and H. Instead of writing the explicit form of H, we write $H = FGF^{\dagger}$ where F is an element of $SU(2)$ as shown below.

$$G = \begin{pmatrix} e^{i\theta} & 0 \\ 0 & e^{-i\theta} \end{pmatrix}$$

$$F = \begin{pmatrix} ic & is \\ is & -ic \end{pmatrix}$$

This representation of braiding where one generator G is a simple matrix of phases, while the other generator $H = FGF^{\dagger}$ is derived from G by conjugation by a unitary matrix, has the possibility for generalization to representations of braid groups (on greater than three strands) to $SU(n)$ or $U(n)$ for n greater than 2. In fact we shall see just such representations [56] by using a version of topological quantum field theory. The simplest example is given by

$$g = e^{7\pi I/10}$$

$$f = I\tau + K\sqrt{\tau}$$

$$h = fgf^{-1}$$

where $\tau^2 + \tau = 1$. Then g and h satisfy $ghg = hgh$ and generate a representation of the three-strand braid group that is dense in $SU(2)$. We shall call this the *Fibonacci* representation of B_3 to $SU(2)$.

At this point we can close this section with the speculation that braid group representations such as this Fibonacci representation can be realized in the context of electrons in nano-wires. The formalism is the same as our basic Majorana representation. It has the form of a braiding operators of the form

$$exp(\theta yx)$$

where x and y are Majorana operators and the angle θ is not equal to $\pi/4$ as is required in the full Majorana representation. For a triple $\{x, y, z\}$ of Majorana operators, any quaternion representation is available. Note how this will effect the conjugation representation: Let $T = r + syx$ where r and s are real numbers with $r^2 + s^2 = 1$ (the cosine and sine of θ), chosen so that a representation of the braid group is formed at the triplet (quaternion level). Then $T^{-1} = r - syx$ and the reader can verify that

$$TxT^{-1} = (r^2 - s^2)x + 2rsy,$$

$$TyT^{-1} = (r^2 - s^2)y - 2rsx.$$

Thus we see that the original Fermion exchange occurs with $r = s$ and then the sign on $-2rs$ is the well-known sign change in the exchange of Fermions. Here it is generalized to a more complex linear combination of the two particle/operators. It remains to be seen what is the meaning of this pattern at the level of Majorana particles in nano-wires.

6 The Bracket Polynomial and the Jones Polynomial

We now discuss the Jones polynomial. We shall construct the Jones polynomial by using the bracket state summation model [32]. The bracket polynomial, invariant under Reidmeister moves II and III, can be normalized to give an invariant of all three Reidemeister moves. This normalized invariant, with a change of variable, is the Jones polynomial [28, 29, 30, 31]. The Jones polynomial was originally discovered by a different method than the one given here.

The *bracket polynomial* , $< K >=< K > (A)$, assigns to each unoriented link diagram K a Laurent polynomial in the variable A, such that

1. If K and K' are regularly isotopic diagrams, then $< K >=< K' >$.

2. If $K \sqcup O$ denotes the disjoint union of K with an extra unknotted and unlinked component O (also called 'loop' or 'simple closed curve' or 'Jordan curve'), then

$$< K \sqcup O >= \delta < K >,$$

where

$$\delta = -A^2 - A^{-2}.$$

3. $< K >$ satisfies the following formulas

$$< \chi >= A < \asymp > +A^{-1} <)(>$$
$$< \overline{\chi} >= A^{-1} < \asymp > +A <)(>,$$

where the small diagrams represent parts of larger diagrams that are identical except at the site indicated in the bracket. We take the convention that the letter chi, χ, denotes a crossing where *the curved line is crossing over the straight segment*. The barred letter denotes the switch of this crossing, where *the curved line is undercrossing the straight segment*. See Figure 6 for a graphic illustration of this relation, and an indication of the convention for choosing the labels A and A^{-1} at a given crossing.

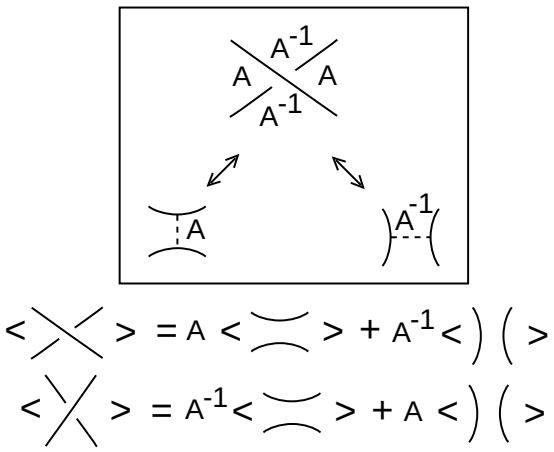

Figure 6: **Bracket Smoothings**

It is easy to see that Properties 2 and 3 define the calculation of the bracket on arbitrary link diagrams. The choices of coefficients (A and A^{-1}) and the value of δ make the bracket invariant under the Reidemeister moves II and III. Thus Property 1 is a consequence of the other two properties.

In computing the bracket, one finds the following behaviour under Reidemeister move I:

$$< \gamma >= -A^3 < \smile >$$

and

$$< \overline{\gamma} >= -A^{-3} < \smile >$$

where γ denotes a curl of positive type as indicated in Figure 7, and $\overline{\gamma}$ indicates a curl of negative type, as also seen in this figure. The type of a curl is the sign of the crossing when we orient it locally. Our convention of signs is also given in Figure 7. Note that the type of a curl does not depend on the orientation we choose. The small arcs on the right hand side of these formulas indicate the removal of the curl from the corresponding diagram.

The bracket is invariant under regular isotopy and can be normalized to an invariant of ambient isotopy by the definition

$$f_K(A) = (-A^3)^{-w(K)} < K > (A),$$

where we chose an orientation for K, and where $w(K)$ is the sum of the crossing signs of the oriented link K. $w(K)$ is called the *writhe* of K. The convention for crossing signs is shown in Figure 7.

One useful consequence of these formulas is the following *switching formula*

$$A < \chi > -A^{-1} < \overline{\chi} >= (A^2 - A^{-2}) < \asymp > .$$

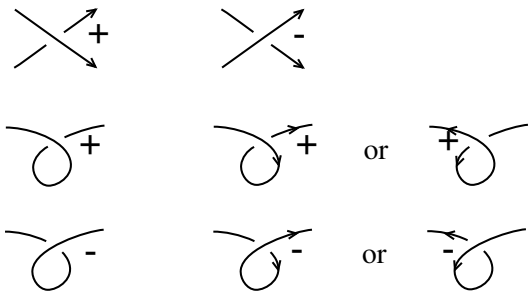

Figure 7: **Crossing Signs and Curls**

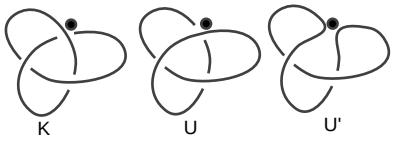

Figure 8: **Trefoil and Two Relatives**

Note that in these conventions the A-smoothing of χ is $\asymp$, while the A-smoothing of $\overline{\chi}$ is $)($. Properly interpreted, the switching formula above says that you can switch a crossing and smooth it either way and obtain a three diagram relation. This is useful since some computations will simplify quite quickly with the proper choices of switching and smoothing. Remember that it is necessary to keep track of the diagrams up to regular isotopy (the equivalence relation generated by the second and third Reidemeister moves). Here is an example. View Figure 8.

Figure 8 shows a trefoil diagram K, an unknot diagram U and another unknot diagram U'. Applying the switching formula, we have

$$A^{-1} < K > -A < U >= (A^{-2} - A^2) < U' >$$

and $< U >= -A^3$ and $< U' >= (-A^{-3})^2 = A^{-6}$. Thus

$$A^{-1} < K > -A(-A^3) = (A^{-2} - A^2)A^{-6}.$$

Hence

$$A^{-1} < K >= -A^4 + A^{-8} - A^{-4}.$$

Thus

$$< K >= -A^5 - A^{-3} + A^{-7}.$$

This is the bracket polynomial of the trefoil diagram K.

Since the trefoil diagram K has writhe $w(K) = 3$, we have the normalized polynomial

$$f_K(A) = (-A^3)^{-3} < K >= -A^{-9}(-A^5 - A^{-3} + A^{-7}) = A^{-4} + A^{-12} - A^{-16}.$$

The bracket model for the Jones polynomial is quite useful both theoretically and in terms of practical computations. One of the neatest applications is to simply compute, as we have done, $f_K(A)$ for the trefoil knot K and determine that $f_K(A)$ is not equal to $f_K(A^{-1}) = f_{-K}(A)$. This shows that the trefoil is not ambient isotopic to its mirror image, a fact that is much harder to prove by classical methods.

The State Summation. In order to obtain a closed formula for the bracket, we now describe it as a state summation. Let K be any unoriented link diagram. Define a *state*, S, of K to be a choice of smoothing for each crossing of K. There are two choices for smoothing a given crossing, and thus there are 2^N states of a diagram with N crossings. In a state we label each smoothing with A or A^{-1} according to the left-right convention discussed in Property 3 (see Figure 6). The label is called a *vertex weight* of the state. There are two evaluations related to a state. The first one is the product of the vertex weights, denoted

$$< K|S > .$$

The second evaluation is the number of loops in the state S, denoted

$$||S||.$$

Define the *state summation*, $< K >$, by the formula

$$< K >= \sum_S < K|S > \delta^{||S||-1}.$$

It follows from this definition that $< K >$ satisfies the equations

$$< \chi >= A < \asymp > +A^{-1} <)(>,$$

$$< K \sqcup O >= \delta < K >,$$

$$< O >= 1.$$

The first equation expresses the fact that the entire set of states of a given diagram is the union, with respect to a given crossing, of those states with an A-type smoothing and those with an A^{-1}-type smoothing at that crossing. The second and the third equation are clear from the formula defining the state summation. Hence this state summation produces the bracket polynomial as we have described it at the beginning of the section.

Remark. By a change of variables one obtains the original Jones polynomial, $V_K(t)$, for oriented knots and links from the normalized bracket:

$$V_K(t) = f_K(t^{-\frac{1}{4}}).$$

Remark. The bracket polynomial provides a connection between knot theory and physics, in that the state summation expression for it exhibits it as a generalized partition function defined on the knot diagram. Partition functions are ubiquitous in statistical mechanics, where they express the summation over all states of the physical system of probability weighting functions for the individual states. Such physical partition functions contain large amounts of information about the corresponding physical system. Some of this information is directly present in the properties of the function, such as the location of critical points and phase transition. Some of the information can be obtained by differentiating the partition function, or performing other mathematical operations on it.

There is much more in this connection with statistical mechanics in that the local weights in a partition function are often expressed in terms of solutions to a matrix equation called the Yang-Baxter equation, that turns out to fit perfectly invariance under the third Reidemeister move. As a result, there are many ways to define partition functions of knot diagrams that give rise to invariants of knots and links. The subject is intertwined with the algebraic structure of Hopf algebras and quantum groups, useful for producing systematic solutions to the Yang-Baxter equation. In fact Hopf algebras are deeply connected with the problem of constructing invariants of three-dimensional manifolds in relation to invariants of knots. We have chosen, in this survey paper, to not discuss the details of these approaches, but rather to proceed to Vassiliev invariants and the relationships with Witten's functional integral. The reader is referred to [32, 33, 34, 35, 37, 38, 29, 30, 39, 79, 80, 83, 84] for more information about relationships of knot theory with statistical mechanics, Hopf algebras and quantum groups. For topology, the key point is that Lie algebras can be used to construct invariants of knots and links.

6.1 Quantum Computation of the Jones Polynomial

Can the invariants of knots and links such as the Jones polynomial be configured as quantum computers? This is an important question because the algorithms to compute the Jones polynomial are known to be $\sharp P$-hard [27], and so corresponding quantum algorithms may shed light on the relationship of this level of computational complexity with quantum computing (See [22]). Such models can be formulated in terms of the Yang-Baxter equation [32, 33, 38, 58, 60]. The next paragraph explains how this comes about.

In Figure 9, we indicate how topological braiding plus maxima (caps) and minima (cups) can be used to configure the diagram of a knot or link. This also can be translated into algebra by the association of a Yang-Baxter matrix R (not necessarily the R of the previous sections) to each crossing and other matrices to the maxima and minima. There are models of very effective invariants of knots and links such as the Jones polynomial that can be put into this form [58, 60].

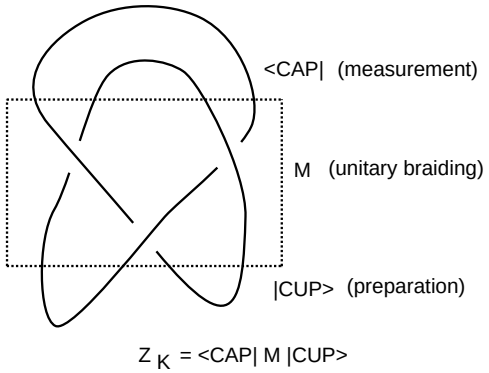

Figure 9: **A Knot Quantum Computer**

In this way of looking at things, the knot diagram can be viewed as a picture, with time as the vertical dimension, of particles arising from the vacuum, interacting (in a two-dimensional space) and finally annihilating one another. The invariant takes the form of an amplitude for this process that is computed through the association of the Yang-Baxter solution R as the scattering matrix at the crossings and the minima and maxima as creation and annihilation operators. Thus we can write the amplitude in the form

$$Z_K = \langle CUP|M|CAP\rangle$$

where $\langle CUP|$ denotes the composition of cups, M is the composition of elementary braiding matrices, and $|CAP\rangle$ is the composition of caps. We regard $\langle CUP|$ as the preparation of this state, and $|CAP\rangle$ as the measurement of this state. In order to view Z_K as a quantum computation, M must be a unitary operator. This is the case when the R-matrices (the solutions to the Yang-Baxter equation used in the model) are unitary. Each R-matrix is viewed as a a quantum gate (or possibly a composition of quantum gates), and the vacuum-vacuum diagram for the knot is interpreted as a quantum computer. This quantum computer will probabilistically (via quantum amplitudes) compute the values of the states in the state sum for Z_K.

We should remark, however, that it is not necessary that the invariant be modeled via solutions to the Yang-Baxter equation. One can use unitary representations of the braid group that are constructed in other ways. In fact, the presently successful quantum algorithms for computing knot invariants indeed use such representations of the braid group, and we shall see this below. Nevertheless, it is useful to point out this analogy between the structure of the knot invariants and quantum computation.

Quantum algorithms for computing the Jones polynomial have been discussed elsewhere. See [58, 59, 55, 1, 60, 2, 87]. Here, as an example, we give a local unitary representation that can be used to compute the Jones polynomial for closures of 3-braids. We analyze this representation by

making explicit how the bracket polynomial is computed from it, and showing how the quantum computation devolves to finding the trace of a unitary transformation.

The idea behind the construction of this representation depends upon the algebra generated by two single qubit density matrices (ket-bras). Let $|v\rangle$ and $|w\rangle$ be two qubits in V, a complex vector space of dimension two over the complex numbers. Let $P = |v\rangle\langle v|$ and $Q = |w\rangle\langle w|$ be the corresponding ket-bras. Note that

$$P^2 = |v|^2 P,$$

$$Q^2 = |w|^2 Q,$$

$$PQP = |\langle v|w\rangle|^2 P,$$

$$QPQ = |\langle v|w\rangle|^2 Q.$$

P and Q generate a representation of the Temperley-Lieb algebra (See Section 9). One can adjust parameters to make a representation of the three-strand braid group in the form

$$s_1 \longmapsto rP + sI,$$

$$s_2 \longmapsto tQ + uI,$$

where I is the identity mapping on V and r, s, t, u are suitably chosen scalars. In the following we use this method to adjust such a representation so that it is unitary. Note also that this is a local unitary representation of B_3 to $U(2)$.

Here is a specific representation depending on two symmetric matrices U_1 and U_2 with

$$U_1 = \begin{bmatrix} d & 0 \\ 0 & 0 \end{bmatrix} = d|w\rangle\langle w|$$

and

$$U_2 = \begin{bmatrix} d^{-1} & \sqrt{1-d^{-2}} \\ \sqrt{1-d^{-2}} & d-d^{-1} \end{bmatrix} = d|v\rangle\langle v|$$

where $w = (1, 0)$, and $v = (d^{-1}, \sqrt{1-d^{-2}})$, assuming the entries of v are real. Note that $U_1^2 = dU_1$ and $U_2^2 = dU_1$. Moreover, $U_1U_2U_1 = U_1$ and $U_2U_1U_2 = U_1$. This is an example of a specific representation of the Temperley-Lieb algebra [32, 58]. The desired representation of the Artin braid group is given on the two braid generators for the three strand braid group by the equations:

$$\Phi(s_1) = AI + A^{-1}U_1,$$
$$\Phi(s_2) = AI + A^{-1}U_2.$$

Here I denotes the 2×2 identity matrix.

For any A with $d = -A^2 - A^{-2}$ these formulas define a representation of the braid group. With $A = e^{i\theta}$, we have $d = -2cos(2\theta)$. We find a specific range of angles θ in the following disjoint union of angular intervals

$$\theta \in [0, \pi/6] \sqcup [\pi/3, 2\pi/3] \sqcup [5\pi/6, 7\pi/6] \sqcup [4\pi/3, 5\pi/3] \sqcup [11\pi/6, 2\pi]$$

that give unitary representations of the three-strand braid group. Thus a specialization of a more general represention of the braid group gives rise to a continuous family of unitary representations of the braid group.

Lemma. Note that the traces of these matrices are given by the formulas $tr(U_1) = tr(U_2) = d$ while $tr(U_1U_2) = tr(U_2U_1) = 1$. If b is any braid, let $I(b)$ denote the sum of the exponents in the braid word that expresses b. For b a three-strand braid, it follows that

$$\Phi(b) = A^{I(b)}I + \Pi(b)$$

where I is the 2×2 identity matrix and $\Pi(b)$ is a sum of products in the Temperley-Lieb algebra involving U_1 and U_2.

We omit the proof of this Lemma. It is a calculation. To see it, consider an example. Suppose that $b = s_1 s_2^{-1} s_1$. Then

$$\Phi(b) = \Phi(s_1 s_2^{-1} s_1) = \Phi(s_1)\Phi(s_2^{-1})\Phi(s_1) =$$

$$(AI + A^{-1}U_1)(A^{-1}I + AU_2)(AI + A^{-1}U_1).$$

The sum of products over the generators U_1 and U_2 of the Temperley–Lieb algebra comes from expanding this expression.

Since the Temperley-Lieb algebra in this dimension is generated by I,U_1, U_2, U_1U_2 and U_2U_1, it follows that the value of the bracket polynomial of the closure of the braid b, denoted $< \overline{b} >$, can be calculated directly from the trace of this representation, except for the part involving the identity matrix. The result is the equation

$$< \overline{b} >= A^{I(b)}d^2 + tr(\Pi(b))$$

where $\overline{b}$ denotes the standard braid closure of b, and the sharp brackets denote the bracket polynomial. From this we see at once that

$$< \overline{b} >= tr(\Phi(b)) + A^{I(b)}(d^2 - 2).$$

It follows from this calculation that the question of computing the bracket polynomial for the closure of the three-strand braid b is mathematically equivalent to the problem of computing the trace of the unitary matrix $\Phi(b)$.

The Hadamard Test

In order to (quantum) compute the trace of a unitary matrix U, one can use the *Hadamard test* to obtain the diagonal matrix elements $\langle\psi|U|\psi\rangle$ of U. The trace is then the sum of these matrix elements as $|\psi\rangle$ runs over an orthonormal basis for the vector space. We first obtain

$$\frac{1}{2} + \frac{1}{2}Re\langle\psi|U|\psi\rangle$$

as an expectation by applying the Hadamard gate H

$$H|0\rangle = \frac{1}{\sqrt{2}}(|0\rangle + |1\rangle)$$

$$H|1\rangle = \frac{1}{\sqrt{2}}(|0\rangle - |1\rangle)$$

to the first qubit of

$$C_U \circ (H \otimes 1)|0\rangle|\psi\rangle = \frac{1}{\sqrt{2}}(|0\rangle \otimes |\psi\rangle + |1\rangle \otimes U|\psi\rangle.$$

Here C_U denotes controlled U, acting as U when the control bit is $|1\rangle$ and the identity mapping when the control bit is $|0\rangle$. We measure the expectation for the first qubit $|0\rangle$ of the resulting state

$$\frac{1}{2}(H|0\rangle \otimes |\psi\rangle + H|1\rangle \otimes U|\psi\rangle) = \frac{1}{2}((|0\rangle + |1\rangle) \otimes |\psi\rangle + (|0\rangle - |1\rangle) \otimes U|\psi\rangle)$$

$$= \frac{1}{2}(|0\rangle \otimes (|\psi\rangle + U|\psi\rangle) + |1\rangle \otimes (|\psi\rangle - U|\psi\rangle)).$$

This expectation is

$$\frac{1}{2}(\langle\psi| + \langle\psi|U^\dagger)(|\psi\rangle + U|\psi\rangle) = \frac{1}{2} + \frac{1}{2}Re\langle\psi|U|\psi\rangle.$$

The imaginary part is obtained by applying the same procedure to

$$\frac{1}{\sqrt{2}}(|0\rangle \otimes |\psi\rangle - i|1\rangle \otimes U|\psi\rangle$$

This is the method used in [1, 2], and the reader may wish to contemplate its efficiency in the context of this simple model. Note that the Hadamard test enables this quantum computation to estimate the trace of any unitary matrix U by repeated trials that estimate individual matrix entries $\langle\psi|U|\psi\rangle$. We shall return to quantum algorithms for the Jones polynomial and other knot polynomials in a subsequent paper.

7 Quantum Topology, Cobordism Categories, Temperley-Lieb Algebra and Topological Quantum Field Theory

The purpose of this section is to discuss the general idea behind topological quantum field theory, and to illustrate its application to basic quantum mechanics and quantum mechanical formalism. It is useful in this regard to have available the concept of *category*, and we shall begin the section by discussing this far-reaching mathematical concept.

Definition. A *category Cat* consists in two related collections:

1. $Obj(Cat)$, the *objects* of Cat, and
2. $Morph(Cat)$, the *morphisms* of Cat.

satisfying the following axioms:

1. Each morphism f is associated to two objects of Cat, the *domain* of f and the *codomain* of f. Letting A denote the domain of f and B denote the codomain of f, it is customary to denote the morphism f by the arrow notation $f : A \longrightarrow B$.
2. Given $f : A \longrightarrow B$ and $g : B \longrightarrow C$ where A, B and C are objects of Cat, then there exists an associated morphism $g \circ f : A \longrightarrow C$ called the *composition* of f and g.
3. To each object A of Cat there is a unique *identity morphism* $1_A : A \longrightarrow A$ such that $1_A \circ f = f$ for any morphism f with codomain A, and $g \circ 1_A = g$ for any morphism g with domain A.
4. Given three morphisms $f : A \longrightarrow B$, $g : B \longrightarrow C$ and $h : C \longrightarrow D$, then composition is associative. That is
$$(h \circ g) \circ f = h \circ (g \circ f).$$

If Cat_1 and Cat_2 are two categories, then a *functor* $F : Cat_1 \longrightarrow Cat_2$ consists in functions $F_O : Obj(Cat_1) \longrightarrow Obj(Cat_2)$ and $F_M : Morph(Cat_1) \longrightarrow Morph(Cat_2)$ such that identity morphisms and composition of morphisms are preserved under these mappings. That is (writing just F for F_O and F_M),

1. $F(1_A) = 1_{F(A)}$,
2. $F(f : A \longrightarrow B) = F(f) : F(A) \longrightarrow F(B)$,
3. $F(g \circ f) = F(g) \circ F(f)$.

A functor $F : Cat_1 \longrightarrow Cat_2$ is a structure preserving mapping from one category to another. It is often convenient to think of the image of the functor F as an *interpretation* of the first category in terms of the second. We shall use this terminology below and sometimes refer to an interpretation without specifying all the details of the functor that describes it.

The notion of category is a broad mathematical concept, encompassing many fields of mathematics. Thus one has the category of sets where the objects are sets (collections) and the morphisms are mappings between sets. One has the category of topological spaces where the objects are spaces and the morphisms are continuous mappings of topological spaces. One has the category of groups where the objects are groups and the morphisms are homomorphisms of groups. Functors are structure preserving mappings from one category to another. For example, the fundamental group is a functor from the category of topological spaces with base point, to the category of groups. In all the examples mentioned so far, the morphisms in the category are restrictions of mappings in the category of sets, but this is not necessarily the case. For example, any group G can be regarded as a category, $Cat(G)$, with one object $*$. The morphisms from $*$ to itself are the elements of the group and composition is group multiplication. In this example, the object has no internal structure and all the complexity of the category is in the morphisms.

The Artin braid group B_n can be regarded as a category whose single object is an ordered row of points $[n] = \{1, 2, 3, ..., n\}$. The morphisms are the braids themselves and composition is the multiplication of the braids. A given ordered row of points is interpreted as the starting or ending row of points at the bottom or the top of the braid. In the case of the braid category, the morphisms have both external and internal structure. Each morphism produces a permutation of the ordered row of points (corresponding to the begiinning and ending points of the individual braid strands), and weaving of the braid is extra structure beyond the object that is its domain and codomain. Finally, for this example, we can take all the braid groups B_n (n a positive integer) under the wing of a single category, $Cat(B)$, whose objects are all ordered rows of points $[n]$, and whose morphisms are of the form $b : [n] \longrightarrow [n]$ where b is a braid in B_n. The reader may wish to have morphisms between objects with different n. We will have this shortly in the Temperley-Lieb category and in the category of tangles.

The *n-Cobordism Category*, $Cob[n]$, has as its objects smooth manifolds of dimension n, and as its morphisms, smooth manifolds M^{n+1} of dimension $n + 1$ with a partition of the boundary, ∂M^{n+1}, into two collections of n-manifolds that we denote by $L(M^{n+1})$ and $R(M^{n+1})$. We regard M^{n+1} as a morphism from $L(M^{n+1})$ to $R(M^{n+1})$

$$M^{n+1} : L(M^{n+1}) \longrightarrow R(M^{n+1}).$$

As we shall see, these cobordism categories are highly significant for quantum mechanics, and the simplest one, $Cob[0]$ is directly related to the Dirac notation of bras and kets and to the Temperley-Lieb algebara. We shall concentrate in this section on these cobordism categories, and their relationships with quantum mechanics.

One can choose to consider either oriented or non-oriented manifolds, and within unoriented manifolds there are those that are orientable and those that are not orientable. In this section we will implicitly discuss only orientable manifolds, but we shall not specify an orientation. In the next section, with the standard definition of topological quantum field theory, the manifolds will be oriented. The definitions of the cobordism categories for oriented manifolds go over mutatis mutandis.

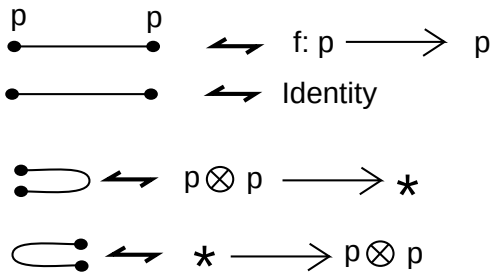

Figure 10: **Elementary Cobordisms**

Lets begin with $Cob[0]$. Zero dimensional manifolds are just collections of points. The simplest zero dimensional manifold is a single point p. We take p to be an object of this category and also $*$, where $*$ denotes the empty manifold (i.e. the empty set in the category of manifolds). The object $*$ occurs in $Cob[n]$ for every n, since it is possible that either the left set or the right set of a morphism is empty. A line segment S with boundary points p and q is a morphism from p to q.

$$S : p \longrightarrow q$$

See Figure 10. In this figure we have illustrated the morphism from p to p. The simplest convention for this category is to take this morphism to be the identity. Thus if we look at the subcategory of $Cob[0]$ whose only object is p, then the only morphism is the identity morphism. Two points occur as the boundary of an interval. The reader will note that $Cob[0]$ and the usual arrow notation for morphisms are very closely related. This is a place where notation and mathematical structure share common elements. In general the objects of $Cob[0]$ consist in the empty object $*$ and non-empty rows of points, symbolized by

$$p \otimes p \otimes \cdots \otimes p \otimes p.$$

Figure 10 also contains a morphism

$$p \otimes p \longrightarrow *$$

and the morphism

$$* \longrightarrow p \otimes p.$$

The first represents a cobordism of two points to the empty set (via the bounding curved interval). The second represents a cobordism from the empty set to two points.

In Figure 11, we have indicated more morphisms in $Cob[0]$, and we have named the morphisms just discussed as

$$|\Omega\rangle : p \otimes p \longrightarrow *,$$

$$\langle\Theta| : * \longrightarrow p \otimes p.$$

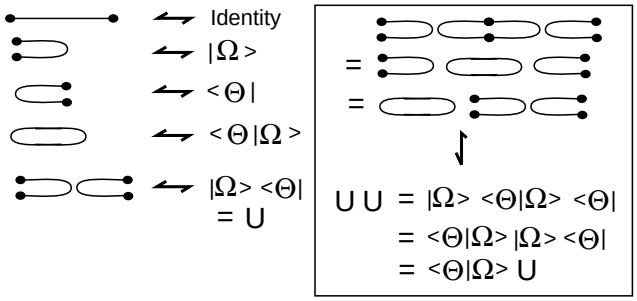

Figure 11: **Bras, Kets and Projectors**

The point to notice is that the usual conventions for handling Dirac bra-kets are essentially the same as the compostion rules in this topological category. Thus in Figure 11 we have that

$$\langle\Theta| \circ |\Omega\rangle = \langle\Theta|\Omega\rangle : * \longrightarrow *$$

represents a cobordism from the empty manifold to itself. This cobordism is topologically a circle and, in the Dirac formalism is interpreted as a scalar. In order to interpret the notion of scalar we would have to map the cobordism category to the category of vector spaces and linear mappings. We shall discuss this after describing the similarities with quantum mechanical formalism. Nevertheless, the reader should note that if V is a vector space over the complex numbers $\mathcal{C}$, then a linear mapping from $\mathcal{C}$ to $\mathcal{C}$ is determined by the image of 1, and hence is characterized by the scalar that is the image of 1. In this sense a mapping $\mathcal{C} \longrightarrow \mathcal{C}$ can be regarded as a possible image in vector spaces of the abstract structure $\langle\Theta|\Omega\rangle : * \longrightarrow *$. It is therefore assumed that in $Cob[0]$ the composition with the morphism $\langle\Theta|\Omega\rangle$ commutes with any other morphism. In that way $\langle\Theta|\Omega\rangle$ behaves like a scalar in the cobordism category. In general, an $n+1$ manifold without boundary behaves as a scalar in $Cob[n]$, and if a manifold M^{n+1} can be written as a union of two submanifolds L^{n+1} and R^{n+1} so that that an n-manifold W^n is their common boundary:

$$M^{n+1} = L^{n+1} \cup R^{n+1}$$

with

$$L^{n+1} \cap R^{n+1} = W^n$$

then, we can write

$$\langle M^{n+1}\rangle = \langle L^{n+1} \cup R^{n+1}\rangle = \langle L^{n+1}|R^{n+1}\rangle,$$

and $\langle M^{n+1}\rangle$ will be a scalar (morphism that commutes with all other morphisms) in the category $Cob[n]$.

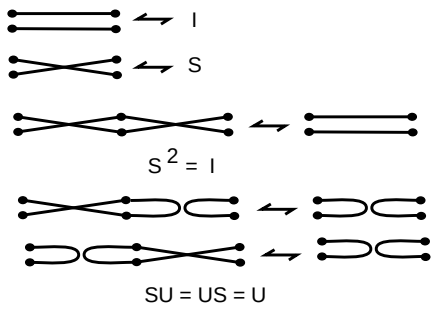

Figure 12: **Permutations**

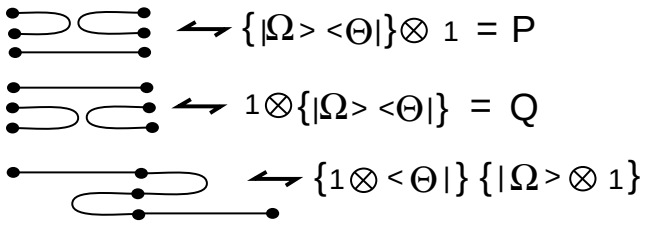

Figure 13: **Projectors in Tensor Lines and Elementary Topology**

Getting back to the contents of Figure 11, note how the zero dimensional cobordism category has structural parallels to the Dirac ket–bra formalism

$$U = |\Omega\rangle\langle\Theta|$$

$$UU = |\Omega\rangle\langle\Theta|\Omega\rangle\langle\Theta| = \langle\Theta|\Omega\rangle|\Omega\rangle\langle\Theta| = \langle\Theta|\Omega\rangle U.$$

In the cobordism category, the bra–ket and ket–bra formalism is seen as patterns of connection of the one-manifolds that realize the cobordisms.

Now view Figure 12. This Figure illustrates a morphism S in $Cob[0]$ that requires two crossed line segments for its planar representation. Thus S can be regarded as a non-trivial permutation, and $S^2 = I$ where I denotes the identity morphisms for a two-point row. From this example, it is clear that $Cob[0]$ contains the structure of all the syymmetric groups and more. In fact, if we take the subcateogry of $Cob[0]$ consisting of all morphisms from $[n]$ to $[n]$ for a fixed positive integer n, then this gives the well-known *Brauer algebra* (see [8]) extending the symmetric group by allowing any connections among the points in the two rows. In this sense, one could call $Cob[0]$ the *Brauer category*. We shall return to this point of view later.

In this section, we shall be concentrating on the part of $Cob[0]$ that does not involve permutations. This part can be characterized by those morphisms that can be represented by planar diagrams without crosssings between any of the line segments (the one-manifolds). We shall call

this crossingless subcategory of $Cob[0]$ the ***Temperley-Lieb Category*** and denote it by $CatTL$. In $CatTL$ we have the subcategory $TL[n]$ whose only objects are the row of n points and the empty object $*$, and whose morphisms can all be represented by configurations that embed in the plane as in the morphisms P and Q in Figure 13. Note that with the empty object $*$, the morphism whose diagram is a single loop appears in $TL[n]$ and is taken to commute with all other morphisms.

The ***Temperley-Lieb Algebra***, $AlgTL[n]$ is generated by the morphisms in $TL[n]$ that go from $[n]$ to itself. Up to multiplication by the loop, the product (composition) of two such morphisms is another flat morphism from $[n]$ to itself. For algebraic purposes the loop $* \longrightarrow *$ is taken to be a scalar algebraic variable δ that commutes with all elements in the algebra. Thus the equation

$$UU = \langle \Theta | \Omega \rangle U.$$

becomes

$$UU = \delta U$$

in the algebra. In the algebra we are allowed to add morphisms formally and this addition is taken to be commutative. Initially the algebra is taken with coefficients in the integers, but a different commutative ring of coefficients can be chosen and the value of the loop may be taken in this ring. For example, for quantum mechanical applications it is natural to work over the complex numbers. The multiplicative structure of $AlgTL[n]$ can be described by generators and relations as follows: Let I_n denote the identity morphism from $[n]$ to $[n]$. Let U_i denote the morphism from $[n]$ to $[n]$ that connects k with k for $k < i$ and $k > i + 1$ from one row to the other, and connects i to $i + 1$ in each row. Then the algebra $AlgTL[n]$ is generated by $\{I_n, U_1, U_2, \cdots, U_{n-1}\}$ with relations

$$U_i^2 = \delta U_i$$

$$U_i U_{i+1} U_i = U_i$$

$$U_i U_j = U_j U_i \ : \ |i - j| > 1.$$

These relations are illustrated for three strands in Figure 13. We leave the commuting relation for the reader to draw in the case where n is four or greater. For a proof that these are indeed all the relations, see [44].

Figure 13 and Figure 14 indicate how the zero dimensional cobordism category contains structure that goes well beyond the usual Dirac formalism. By tensoring the ket–bra on one side or another by identity morphisms, we obtain the beginnings of the Temperley-Lieb algebra and the Temperley-Lieb category. Thus Figure 14 illustrates the morphisms P and Q obtained by such tensoring, and the relation $PQP = P$ which is the same as $U_1 U_2 U_1 = U_1$

Note the composition at the bottom of the Figure 14. Here we see a composition of the identity tensored with a ket, followed by a bra tensored with the identity. The diagrammatic for this association involves "straightening" the curved structure of the morphism to a straight line. In Figure 15 we have elaborated this situation even further, pointing out that in this category each

of the morphisms $\langle\Theta|$ and $|\Omega\rangle$ can be seen, by straightening, as mappings from the generating object to itself. We have denoted these corresponding morphisms by Θ and Ω respectively. In this way there is a correspondence between morphisms $p \otimes p \longrightarrow *$ and morphims $p \longrightarrow p$.

In Figure 15 we have illustrated the generalization of the straightening procedure of Figure 14. In Figure 14 the straightening occurs because the connection structure in the morphism of $Cob[0]$ does not depend on the wandering of curves in diagrams for the morphisms in that category. Nevertheless, one can envisage a more complex interpretation of the morphisms where each one-manifold (line segment) has a label, and a multiplicity of morphisms can correspond to a single line segment. This is exactly what we expect in interpretations. For example, we can interpret the line segment $[1] \longrightarrow [1]$ as a mapping from a vector space V to itself. Then $[1] \longrightarrow [1]$ is the diagrammatic abstraction for $V \longrightarrow V$, and there are many instances of linear mappings from V to V.

At the vector space level there is a duality between mappings $V \otimes V \longrightarrow \mathcal{C}$ and linear maps $V \longrightarrow V$. Specifically, let

$$\{|0\rangle, \cdots, |m\rangle\}$$

be a basis for V. Then $\Theta : V \longrightarrow V$ is determined by

$$\Theta|i\rangle = \Theta_{ij}\,|j\rangle$$

(where we have used the Einstein summation convention on the repeated index j) corresponds to the bra

$$\langle\Theta| : V \otimes V \longrightarrow \mathcal{C}$$

defined by

$$\langle\Theta|ij\rangle = \Theta_{ij}.$$

Given $\langle\Theta| : V \otimes V \longrightarrow \mathcal{C}$, we associate $\Theta : V \longrightarrow V$ in this way.

Comparing with the diagrammatic for the category $Cob[0]$, we say that $\Theta : V \longrightarrow V$ is obtained by *straightening* the mapping

$$\langle\Theta| : V \otimes V \longrightarrow \mathcal{C}.$$

Note that in this interpretation, the bras and kets are defined relative to the tensor product of V with itself and $[2]$ is interpreted as $V \otimes V$. If we interpret $[2]$ as a single vector space W, then the usual formalisms of bras and kets still pass over from the cobordism category.

Figure 15 illustrates the staightening of $|\Theta\rangle$ and $\langle\Omega|$, and the straightening of a composition of these applied to $|\psi\rangle$, resulting in $|\phi\rangle$. In the left-hand part of the bottom of Figure 15 we illustrate the preparation of the tensor product $|\Theta\rangle \otimes |\psi\rangle$ followed by a successful measurement by $\langle\Omega|$ in the second two tensor factors. The resulting single qubit state, as seen by straightening, is $|\phi\rangle = \Theta \circ \Omega|\psi\rangle$.

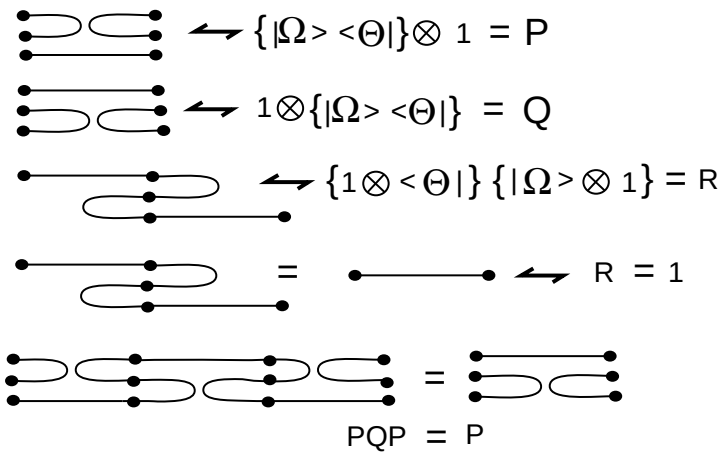

Figure 14: **The Basic Temperley-Lieb Relation**

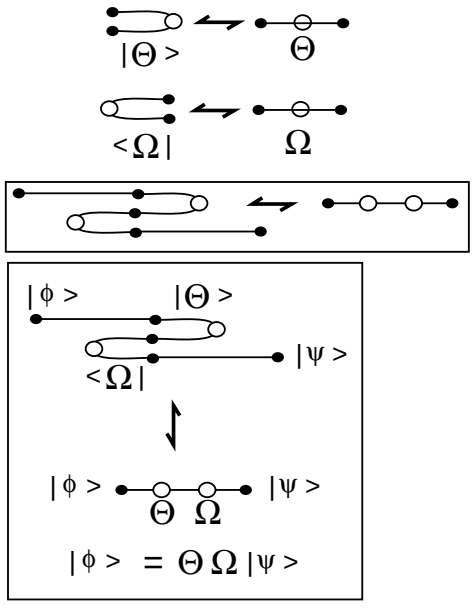

Figure 15: **The Key to Teleportation**

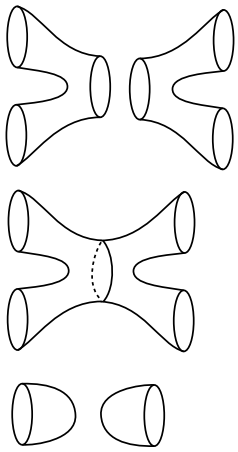

Figure 16: **Corbordisms of 1-Manifolds are Surfaces**

From this, we see that it is possible to reversibly, indeed unitarily, transform a state $|\psi\rangle$ via a combination of preparation and measurement just so long as the straightenings of the preparation and measurement (Θ and Ω) are each invertible (unitary). This is the key to teleportation [43, 15, 16]. In the standard teleportation procedure one chooses the preparation Θ to be (up to normalization) the 2 dimensional identity matrix so that $|\theta\rangle = |00\rangle + |11\rangle$. If the successful measurement Ω is also the identity, then the transmitted state $|\phi\rangle$ will be equal to $|\psi\rangle$. In general we will have $|\phi\rangle = \Omega|\psi\rangle$. One can then choose a basis of measurements $|\Omega\rangle$, each corresponding to a unitary transformation Ω so that the recipient of the transmission can rotate the result by the inverse of Ω to reconsitute $|\psi\rangle$ if he is given the requisite information. This is the basic design of the teleportation procedure.

There is much more to say about the category $Cob[0]$ and its relationship with quantum mechanics. We will stop here, and invite the reader to explore further. Later in this paper, we shall use these ideas in formulating our representations of the braid group. For now, we point out how things look as we move upward to $Cob[n]$ for $n > 0$. In Figure 16 we show typical cobordisms (morphisms) in $Cob[1]$ from two circles to one circle and from one circle to two circles. These are often called "pairs of pants". Their composition is a surface of genus one seen as a morphism from two circles to two circles. The bottom of the figure indicates a ket-bra in this dimension in the form of a mapping from one circle to one circle as a composition of a cobordism of a circle to the empty set and a cobordism from the empty set to a circle (circles bounding disks). As we go to higher dimensions the structure of cobordisms becomes more interesting and more complicated. It is remarkable that there is so much structure in the lowest dimensions of these categories.

8 Braiding and Topological Quantum Field Theory

The purpose of this section is to discuss in a very general way how braiding is related to topological quantum field theory. In the section to follow, we will use the Temperley-Lieb recoupling theory to produce specfic unitary representations of the Artin braid group.

The ideas in the subject of topological quantum field theory (TQFT) are well expressed in the book [5] by Michael Atiyah and the paper [86] by Edward Witten. Here is Atiyah's definition:

Definition. A TQFT in dimension d is a functor $Z(\Sigma)$ from the cobordism category $Cob[d]$ to the category $Vect$ of vector spaces and linear mappings which assigns

1. a finite dimensional vector space $Z(\Sigma)$ to each compact, oriented d-dimensional manifold Σ,

2. a vector $Z(Y) \in Z(\Sigma)$ for each compact, oriented $(d+1)$-dimensional manifold Y with boundary Σ.

3. a linear mapping $Z(Y) : Z(\Sigma_1) \longrightarrow Z(\Sigma_2)$ when Y is a $(d+1)$-manifold that is a cobordism between Σ_1 and Σ_2 (whence the boundary of Y is the union of Σ_1 and $-\Sigma_2$.

The functor satisfies the following axioms.

1. $Z(\Sigma^{\dagger}) = Z(\Sigma)^{\dagger}$ where $\Sigma^{\dagger}$ denotes the manifold Σ with the opposite orientation and $Z(\Sigma)^{\dagger}$ is the dual vector space.

2. $Z(\Sigma_1 \cup \Sigma_2) = Z(\Sigma_1) \otimes Z(\Sigma_2)$ where $\cup$ denotes disjoint union.

3. If Y_1 is a cobordism from Σ_1 to Σ_2, Y_2 is a cobordism from Σ_2 to Σ_3 and Y is the composite cobordism $Y = Y_1 \cup_{\Sigma_2} Y_2$, then

$$Z(Y) = Z(Y_2) \circ Z(Y_1) : Z(\Sigma_1) \longrightarrow Z(\Sigma_2)$$

   is the composite of the corresponding linear mappings.

4. $Z(\phi) = \mathcal{C}$ ($\mathcal{C}$ denotes the complex numbers) for the empty manifold ϕ.

5. With $\Sigma \times I$ (where I denotes the unit interval) denoting the identity cobordism from Σ to Σ, $Z(\Sigma \times I)$ is the identity mapping on $Z(\Sigma)$.

Note that, in this view a TQFT is basically a functor from the cobordism categories defined in the last section to Vector Spaces over the complex numbers. We have already seen that in the lowest dimensional case of cobordisms of zero-dimensional manifolds, this gives rise to a rich structure related to quatum mechanics and quantum information theory. The remarkable fact is that the case of three-dimensions is also related to quantum theory, and to the lower-dimensional versions of the TQFT. This gives a significant way to think about three-manifold invariants in terms of lower dimensional patterns of interaction. Here follows a brief description.

Regard the three-manifold as a union of two handlebodies with boundary an orientable surface S_g of genus g. The surface is divided up into trinions as illustrated in Figure 17. A *trinion* is a surface with boundary that is topologically equivalent to a sphere with three punctures. The trinion constitutes, in itself a cobordism in $Cob[1]$ from two circles to a single circle, or from a single circle to two circles, or from three circles to the empty set. The *pattern* of a trinion is a trivalent graphical vertex, as illustrated in Figure 17. In that figure we show the trivalent vertex graphical pattern drawn on the surface of the trinion, forming a graphical pattern for this combordism. It should be clear from this figure that any cobordism in $Cob[1]$ can be diagrammed by a trivalent graph, so that the category of trivalent graphs (as morphisms from ordered sets of points to ordered sets of points) has an image in the category of cobordisms of compact one-dimensional manifolds. Given a surface S (possibly with boundary) and a decomposition of that surface into triions, we associate to it a trivalent graph $G(S,t)$ where t denotes the particular trinion decomposition.

In this correspondence, distinct graphs can correspond to topologically identical cobordisms of circles, as illustrated in Figure 19. It turns out that the graphical structure is important, and that it is extraordinarily useful to articulate transformations between the graphs that correspond to the homeomorphisms of the corresponding surfaces. The beginning of this structure is indicated in the bottom part of Figure 19.

In Figure 20 we illustrate another feature of the relationship betweem surfaces and graphs. At the top of the figure we indicate a homeomorphism between a twisted trinion and a standard trinion. The homeomorphism leaves the ends of the trinion (denoted A,B and C) fixed while undoing the internal twist. This can be accomplished as an ambient isotopy of the embeddings in three dimensional space that are indicated by this figure. Below this isotopy we indicate the corresponding graphs. In the graph category there will have to be a transformation between a braided and an unbraided trivalent vertex that corresponds to this homeomorphism.

From the point of view that we shall take in this paper, the key to the mathematical structure of three-dimensional TQFT lies in the trivalent graphs, including the braiding of grapical arcs. We can think of these braided graphs as representing idealized Feynman diagrams, with the trivalent vertex as the basic particle interaction vertex, and the braiding of lines representing an interaction resulting from an exchange of particles. In this view one thinks of the particles as moving in a two-dimensional medium, and the diagrams of braiding and trivalent vertex interactions as indications of the temporal events in the system, with time indicated in the direction of the morphisms in the category. Adding such graphs to the category of knots and links is an extension of the *tangle category* where one has already extended braids to allow any embedding of strands and circles that start in n ordered points and end in m ordered points. The tangle category includes the braid category and the Temperley-Lieb category. These are both included in the category of braided trivalent graphs.

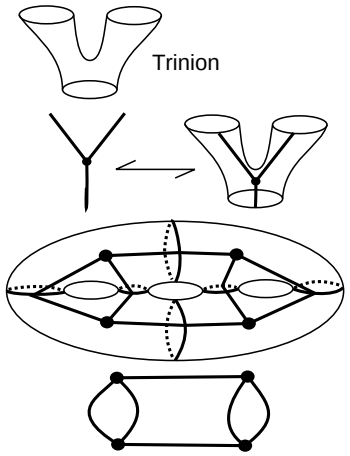

Figure 17: **Decomposition of a Surface into Trinions**

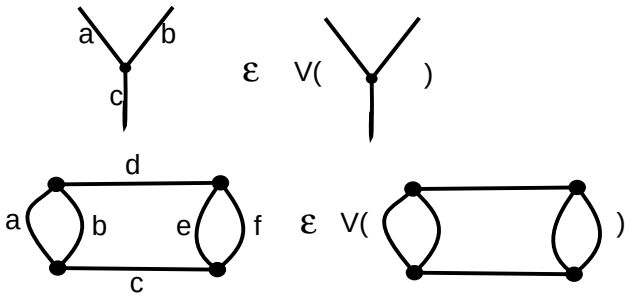

Figure 18: **Trivalent Vectors**

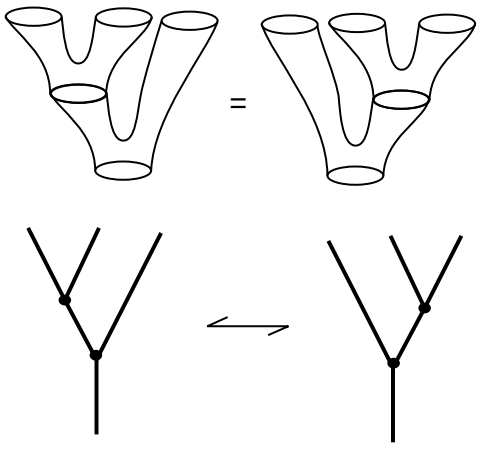

Figure 19: **Trinion Associativity**

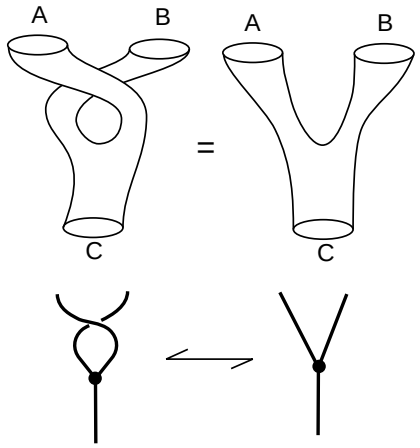

Figure 20: **Tube Twist**

Thinking of the basic trivalent vertex as the form of a particle interaction there will be a set of particle states that can label each arc incident to the vertex. In Figure 18 we illustrate the labeling of the trivalent graphs by such particle states. In the next two sections we will see specific rules for labeling such states. Here it suffices to note that there will be some restrictions on these labels, so that a trivalent vertex has a set of possible labelings. Similarly, any trivalent graph will have a set of admissible labelings. These are the possible particle processes that this graph can support. We take the set of admissible labelings of a given graph G as a basis for a vector space $V(G)$ over the complex numbers. This vector space is the space of *processes* associated with the graph G. Given a surface S and a decomposition t of the surface into trinions, we have the associated graph $G(S,t)$ and hence a vector space of processes $V(G(S,t))$. It is desirable to have this vector space independent of the particular decomposition into trinions. If this can be accomplished, then the set of vector spaces and linear mappings associated to the surfaces can consitute a functor from the category of cobordisms of one-manifolds to vector spaces, and hence gives rise to a one-dimensional topological quantum field theory. To this end we need some properties of the particle interactions that will be described below.

A *spin network* is, by definition a lableled trivalent graph in a category of graphs that satisfy the properties outlined in the previous paragraph. We shall detail the requirements below.

The simplest case of this idea is C. N. Yang's original interpretation of the Yang-Baxter equation [88]. Yang articulated a quantum field theory in one dimension of space and one dimension of time in which the R-matrix giving the scattering ampitudes for an interaction of two particles whose (let us say) spins corresponded to the matrix indices so that R_{ab}^{cd} is the amplitude for particles of spin a and spin b to interact and produce particles of spin c and d. Since these interactions are between particles in a line, one takes the convention that the particle with spin a is to the left of the particle with spin b, and the particle with spin c is to the left of the particle with spin d. If one follows the concatenation of such interactions, then there is an underlying permutation that

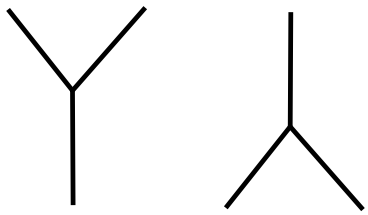

Figure 21: **Creation and Fusion**

is obtained by following strands from the bottom to the top of the diagram (thinking of time as moving up the page). Yang designed the Yang-Baxter equation for R so that *the amplitudes for a composite process depend only on the underlying permutation corresponding to the process and not on the individual sequences of interactions.*

In taking over the Yang-Baxter equation for topological purposes, we can use the same interpretation, but think of the diagrams with their under- and over-crossings as modeling events in a spacetime with two dimensions of space and one dimension of time. The extra spatial dimension is taken in displacing the woven strands perpendicular to the page, and allows us to use braiding operators R and R^{-1} as scattering matrices. Taking this picture to heart, one can add other particle properties to the idealized theory. In particular one can add fusion and creation vertices where in fusion two particles interact to become a single particle and in creation one particle changes (decays) into two particles. These are the trivalent vertices discussed above. Matrix elements corresponding to trivalent vertices can represent these interactions. See Figure 21.

Once one introduces trivalent vertices for fusion and creation, there is the question how these interactions will behave in respect to the braiding operators. There will be a matrix expression for the compositions of braiding and fusion or creation as indicated in Figure 25. Here we will restrict ourselves to showing the diagrammatics with the intent of giving the reader a flavor of these structures. It is natural to assume that braiding intertwines with creation as shown in Figure 24 (similarly with fusion). This intertwining identity is clearly the sort of thing that a topologist will love, since it indicates that the diagrams can be interpreted as embeddings of graphs in three-dimensional space, and it fits with our interpretation of the vertices in terms of trinions. Figure 22 illustrates the Yang-Baxter equation. The intertwining identity is an assumption like the Yang-Baxter equation itself, that simplifies the mathematical structure of the model.

It is to be expected that there will be an operator that expresses the recoupling of vertex interactions as shown in Figure 25 and labeled by Q. This corresponds to the associativity at the level of trinion combinations shown in Figure 19. The actual formalism of such an operator will parallel the mathematics of recoupling for angular momentum. See for example [34]. If one just

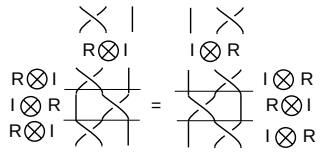

Figure 22: **Yang Baxter Equation**

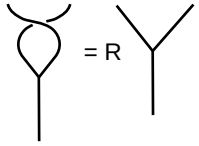

Figure 23: **Braiding**

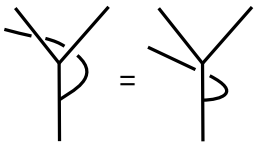

Figure 24: **Intertwining**

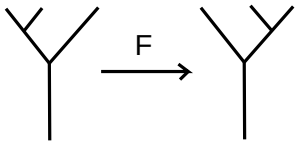

Figure 25: **Recoupling**

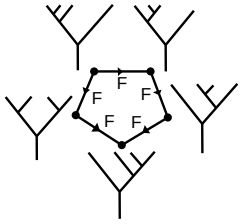

Figure 26: **Pentagon Identity**

considers the abstract structure of recoupling then one sees that for trees with four branches (each with a single root) there is a cycle of length five as shown in Figure 26. One can start with any pattern of three vertex interactions and go through a sequence of five recouplings that bring one back to the same tree from which one started. *It is a natural simplifying axiom to assume that this composition is the identity mapping.* This axiom is called the *pentagon identity*.

Finally there is a hexagonal cycle of interactions between braiding, recoupling and the intertwining identity as shown in Figure 27. One says that the interactions satisfy the *hexagon identity* if this composition is the identity.

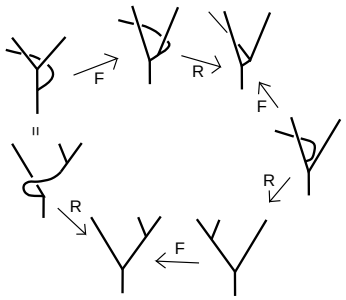

Figure 27: **Hexagon Identity**

Remark. It is worth pointing out how these identities are related to the braiding. The hexagon identity tells us that

$$R^{-1}FRF^{-1}RF = I$$

where I is the identity mapping on the process space for trees with three branches. Letting

$$A = R$$

and

$$B = F^{-1}RF,$$

we see that the hexagon identity is equivalent to the statement

$$B = R^{-1}F^{-1}R.$$

Thus

$$ABA = R(R^{-1}F^{-1}R)R = F^{-1}R^2 = (F^{-1}RF)F^{-1}R = (R^{-1}F^{-1}R)F^{-1}R$$

$$= (R^{-1}F^{-1}R)R(R^{-1}F^{-1}R) = BAB.$$

Thus the hexagon relation in this context, implies that A and B satisfy the braiding relation. The combination of the hexagon and pentagon relations ensures that the braid group representations that are generated are well-defined and fit together as we include smaller numbers of strands in larger numbers of strands. We omit the further details of the verification of this statement.

A *graphical three-dimensional topological quantum field theory* is an algebra of interactions that satisfies the Yang-Baxter equation, the intertwining identity, the pentagon identity and the hexagon identity. There is not room in this summary to detail the way that these properties fit into the topology of knots and three-dimensional manifolds, but a sketch is in order. For the case of topological quantum field theory related to the group $SU(2)$ there is a construction based entirely on the combinatorial topology of the bracket polynomial (See Sections 11 to 13 of this paper.). See [38, 34] for more information on this approach.

Now return to Figure 17 where we illustrate trinions, shown in relation to a trivalent vertex, and a surface of genus three that is decomposed into four trinions. It turns out that the vector space $V(S_g) = V(G(S_g, t))$ to a surface with a trinion decomposition as t described above, and defined in terms of the graphical topological quantum field theory, does not depend upon the choice of trinion decomposition. This independence is guaranteed by the braiding, hexagon and pentagon identities. One can then associate a well-defined vector $|M\rangle$ in $V(S_g)$ whenenver M is a three manifold whose boundary is S_g. Furthermore, if a closed three-manifold M^3 is decomposed along a surface S_g into the union of M_- and M_+ where these parts are otherwise disjoint three-manifolds with boundary S_g, then the inner product $I(M) = \langle M_-|M_+\rangle$ is, up to normalization, an invariant of the three-manifold M_3. With the definition of graphical topological quantum field theory given above, knots and links can be incorporated as well, so that one obtains a source of invariants $I(M^3, K)$ of knots and links in orientable three-manifolds. Here we see the uses of the relationships that occur in the higher dimensional cobordism categories, as descirbed in the previous section.

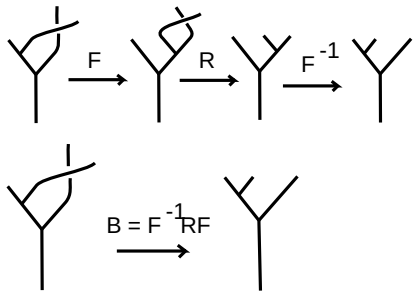

Figure 28: **A More Complex Braiding Operator**

The invariant $I(M^3, K)$ can be formally compared with the Witten [86] integral

$$Z(M^3, K) = \int DA e^{(ik/4\pi)S(M,A)} W_K(A).$$

It can be shown that up to limits of the heuristics, $Z(M, K)$ and $I(M^3, K)$ are essentially equivalent for appropriate choice of gauge group and corresponding spin networks.

By these graphical reformulations, a three-dimensional $TQFT$ is, at base, a highly simplified theory of point particle interactions in $2 + 1$ dimensional spacetime. It can be used to articulate invariants of knots and links and invariants of three manifolds. The reader interested in the $SU(2)$ case of this structure and its implications for invariants of knots and three manifolds can consult [34, 38, 66, 14]. One expects that physical situations involving $2 + 1$ spacetime will be approximated by such an idealized theory. There are also applications to $3 + 1$ quantum gravity [45]. Aspects of the quantum Hall effect may be related to topological quantum field theory [85]. One can study a physics in two dimensional space where the braiding of particles or collective excitations leads to non-trival representations of the Artin braid group. Such particles are called *Anyons*. Such $TQFT$ models would describe applicable physics. One can think about applications of anyons to quantum computing along the lines of the topoological models described here.

A key point in the application of $TQFT$ to quantum information theory is contained in the structure illustrated in Figure 28. There we show a more complex braiding operator, based on the composition of recoupling with the elementary braiding at a vertex. (This structure is implicit in the Hexagon identity of Figure 27.) The new braiding operator is a source of unitary representations of braid group in situations (which exist mathematically) where the recoupling transformations are themselves unitary. This kind of pattern is utilized in the work of Freedman and collaborators [20, 21, 22, 23, 24] and in the case of classical angular momentum formalism has been dubbed a "spin-network quantum simlator" by Rasetti and collaborators [70, 71]. In the next section we show how certain natural deformations [34] of Penrose spin networks [77] can be used to produce these unitary representations of the Artin braid group and the corresponding models for anyonic topological quantum computation.

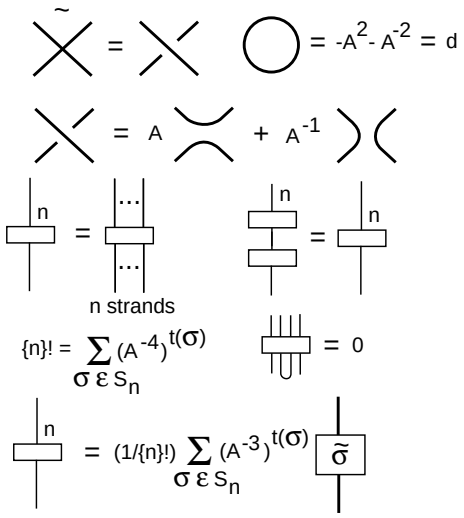

Figure 29: **Basic Projectors**

9 Spin Networks and Temperley-Lieb Recoupling Theory

In this section we discuss a combinatorial construction for spin networks that generalizes the original construction of Roger Penrose. The result of this generalization is a structure that satisfies all the properties of a graphical $TQFT$ as described in the previous section, and specializes to classical angular momentum recoupling theory in the limit of its basic variable. The construction is based on the properties of the bracket polynomial (as already described in Section 6). A complete description of this theory can be found in the book "Temperley-Lieb Recoupling Theory and Invariants of Three-Manifolds" by Kauffman and Lins [34].

The "q-deformed" spin networks that we construct here are based on the bracket polynomial relation. View Figure 29 and Figure 30.

In Figure 29 we indicate how the basic projector $\dot{+}$ (symmetrizer, Jones-Wenzl projector) is constructed on the basis of the bracket polynomial expansion. In this technology a symmetrizer is a sum of tangles on n strands (for a chosen integer n). The tangles are made by summing over braid lifts of permutations in the symmetric group on n letters, as indicated in Figure 29. Each elementary braid is then expanded by the bracket polynomial relation as indicated in Figure 29 so that the resulting sum consists of flat tangles without any crossings (these can be viewed as elements in the Temperley-Lieb algebra). The projectors have the property that the concatenation of a projector with itself is just that projector, and if you tie two lines on the top or the bottom of a projector together, then the evaluation is zero. This general definition of projectors is very

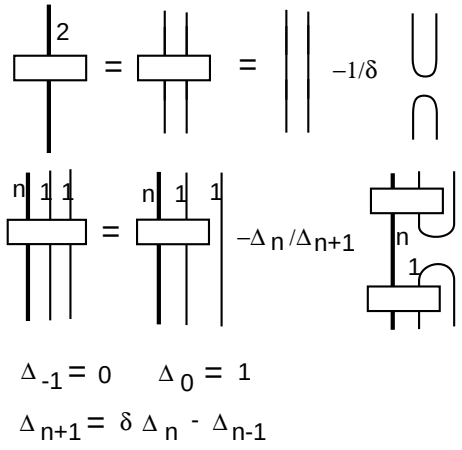

Figure 30: **Two Strand Projector**

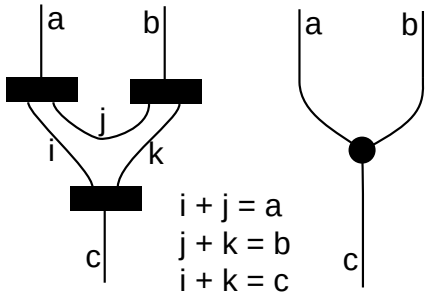

Figure 31: **Vertex**

useful for this theory. The two-strand projector is shown in Figure 30. Here the formula for that projector is particularly simple. It is the sum of two parallel arcs and two turn-around arcs (with coefficient $-1/d$, with $d = -A^2 - A^{-2}$ is the loop value for the bracket polynomial. Figure 30 also shows the recursion formula for the general projector. This recursion formula is due to Jones and Wenzl and the projector in this form, developed as a sum in the Temperley–Lieb algebra (see Section 9 of this paper), is usually known as the *Jones–Wenzl projector*.

The projectors are combinatorial analogs of irreducible representations of a group (the original spin nets were based on $SU(2)$ and these deformed nets are based on the corresponding quantum group to SU(2)). As such the reader can think of them as "particles". The interactions of these particles are governed by how they can be tied together into three-vertices. See Figure 31. In Figure 31 we show how to tie three projectors, of a, b, c strands respectively, together to form a three-vertex. In order to accomplish this interaction, we must share lines between them as shown in that figure so that there are non-negative integers i, j, k so that $a = i + j, b = j + k, c = i + k$. This is equivalent to the condition that $a + b + c$ is even and that the sum of any two of a, b, c is greater than or equal to the third. For example $a + b \geq c$. One can think of the vertex as a possible particle interaction where $[a]$ and $[b]$ interact to produce $[c]$. That is, any two of the legs of the vertex can be regarded as interacting to produce the third leg.

There is a basic orthogonality of three vertices as shown in Figure 32. Here if we tie two three-vertices together so that they form a "bubble" in the middle, then the resulting network with labels a and b on its free ends is a multiple of an a-line (meaning a line with an a-projector on it) or zero (if a is not equal to b). The multiple is compatible with the results of closing the diagram in the equation of Figure 32 so the two free ends are identified with one another. On closure, as shown in the figure, the left hand side of the equation becomes a Theta graph and the right hand side becomes a multiple of a "delta" where Δ_a denotes the bracket polynomial evaluation of the a-strand loop with a projector on it. The $\Theta(a, b, c)$ denotes the bracket evaluation of a theta graph made from three trivalent vertices and labeled with a, b, c on its edges.

There is a recoupling formula in this theory in the form shown in Figure 33. Here there are "6-j symbols", recoupling coefficients that can be expressed, as shown in Figure 33, in terms of tetrahedral graph evaluations and theta graph evaluations. The tetrahedral graph is shown in Figure 34. One derives the formulas for these coefficients directly from the orthogonality relations for the trivalent vertices by closing the left hand side of the recoupling formula and using orthogonality to evaluate the right hand side. This is illustrated in Figure 35. The reader should be advised that there are specific calculational formulas for the theta and tetrahedral nets. These can be found in [34]. Here we are indicating only the relationships and external logic of these objects.

Finally, there is the braiding relation, as illustrated in Figure 33.

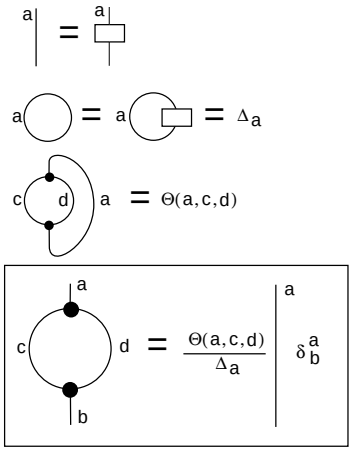

Figure 32: **Orthogonality of Trivalent Vertices**

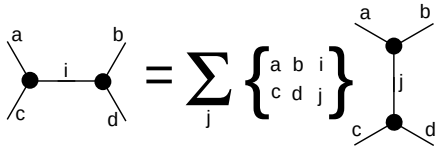

Figure 33: **Recoupling Formula**

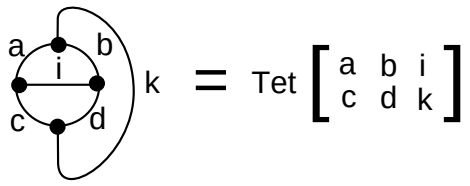

Figure 34: **Tetrahedron Network**

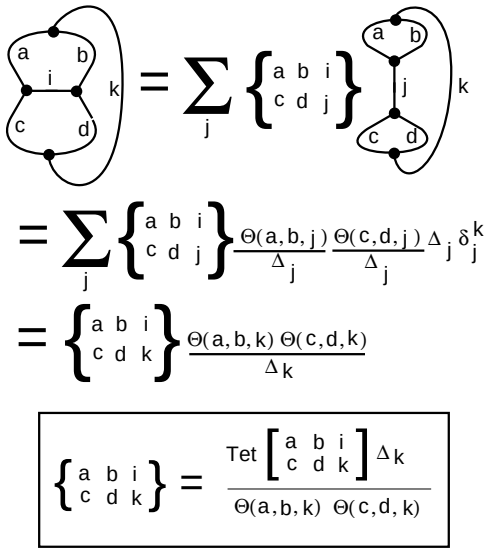

Figure 35: **Tetrahedron Formula for Recoupling Coefficients**

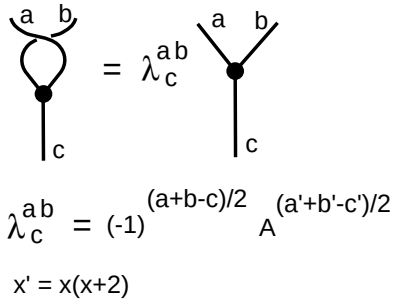

Figure 36: **Local Braiding Formula**

With the braiding relation in place, this q-deformed spin network theory satisfies the pentagon, hexagon and braiding naturality identities needed for a topological quantum field theory. All these identities follow naturally from the basic underlying topological construction of the bracket polynomial. One can apply the theory to many different situations.

9.1 Evaluations

In this section we discuss the structure of the evaluations for Δ_n and the theta and tetrahedral networks. We refer to [34] for the details behind these formulas. Recall that Δ_n is the bracket evaluation of the closure of the n-strand projector, as illustrated in Figure 32. For the bracket variable A, one finds that

$$\Delta_n = (-1)^n \frac{A^{2n+2} - A^{-2n-2}}{A^2 - A^{-2}}.$$

One sometimes writes the *quantum integer*

$$[n] = (-1)^{n-1}\Delta_{n-1} = \frac{A^{2n} - A^{-2n}}{A^2 - A^{-2}}.$$

If

$$A = e^{i\pi/2r}$$

where r is a positive integer, then

$$\Delta_n = (-1)^n \frac{sin((n+1)\pi/r)}{sin(\pi/r)}.$$

Here the corresponding quantum integer is

$$[n] = \frac{sin(n\pi/r)}{sin(\pi/r)}.$$

Note that $[n+1]$ is a positive real number for $n = 0, 1, 2, ...r-2$ and that $[r-1] = 0$.

The evaluation of the theta net is expressed in terms of quantum integers by the formula

$$\Theta(a,b,c) = (-1)^{m+n+p} \frac{[m+n+p+1]![n]![m]![p]!}{[m+n]![n+p]![p+m]!}$$

where

$$a = m+p, b = m+n, c = n+p.$$

Note that

$$(a+b+c)/2 = m+n+p.$$

When $A = e^{i\pi/2r}$, the recoupling theory becomes finite with the restriction that only three-vertices (labeled with a, b, c) are *admissible* when $a+b+c \leq 2r-4$. All the summations in the formulas for recoupling are restricted to admissible triples of this form.

9.2 Symmetry and Unitarity

The formula for the recoupling coefficients given in Figure 35 has less symmetry than is actually inherent in the structure of the situation. By multiplying all the vertices by an appropriate factor, we can reconfigure the formulas in this theory so that the revised recoupling transformation is orthogonal, in the sense that its transpose is equal to its inverse. This is a very useful fact. It means that when the resulting matrices are real, then the recoupling transformations are unitary. We shall see particular applications of this viewpoint later in the paper.

Figure 37 illustrates this modification of the three-vertex. Let $Vert[a, b, c]$ denote the original 3-vertex of the Temperley-Lieb recoupling theory. Let $ModVert[a, b, c]$ denote the modified vertex. Then we have the formula

$$ModVert[a, b, c] = \frac{\sqrt{\sqrt{\Delta_a \Delta_b \Delta_c}}}{\sqrt{\Theta(a, b, c)}}\ Vert[a, b, c].$$

Lemma. For the bracket evaluation at the root of unity $A = e^{i\pi/2r}$ the factor

$$f(a, b, c) = \frac{\sqrt{\sqrt{\Delta_a \Delta_b \Delta_c}}}{\sqrt{\Theta(a, b, c)}}$$

is real, and can be taken to be a positive real number for (a, b, c) admissible (i.e. $a+b+c \leq 2r-4$).

Proof. By the results from the previous subsection,

$$\Theta(a, b, c) = (-1)^{(a+b+c)/2}\hat{\Theta}(a, b, c)$$

where $\hat{\Theta}(a, b, c)$ is positive real, and

$$\Delta_a \Delta_b \Delta_c = (-1)^{(a+b+c)}[a + 1][b + 1][c + 1]$$

where the quantum integers in this formula can be taken to be positive real. It follows from this that

$$f(a, b, c) = \sqrt{\frac{\sqrt{[a + 1][b + 1][c + 1]}}{\hat{\Theta}(a, b, c)}},$$

showing that this factor can be taken to be positive real. //

In Figure 38 we show how this modification of the vertex affects the non-zero term of the orthogonality of trivalent vertices (compare with Figure 32). We refer to this as the "modified bubble identity." The coefficient in the modified bubble identity is

$$\sqrt{\frac{\Delta_b \Delta_c}{\Delta_a}} = (-1)^{(b+c-a)/2}\sqrt{\frac{[b + 1][c + 1]}{[a + 1]}}$$

where (a, b, c) form an admissible triple. In particular $b + c - a$ is even and hence this factor can be taken to be real.

We rewrite the recoupling formula in this new basis and emphasize that the recoupling coefficients can be seen (for fixed external labels a, b, c, d) as a matrix transforming the horizontal "double-Y" basis to a vertically disposed double-Y basis. In Figure 39, Figure 40 and Figure 41 we have shown the form of this transformation,using the matrix notation

$$M[a, b, c, d]_{ij}$$

for the modified recoupling coefficients. In Figure 39 we derive an explicit formula for these matrix elements. The proof of this formula follows directly from trivalent–vertex orthogonality (See Figure 32 and Figure 35.), and is given in Figure 39. The result shown in Figure 39 and Figure 40 is the following formula for the recoupling matrix elements.

$$M[a, b, c, d]_{ij} = ModTet \begin{pmatrix} a & b & i \\ c & d & j \end{pmatrix} / \sqrt{\Delta_a \Delta_b \Delta_c \Delta_d}$$

where $\sqrt{\Delta_a \Delta_b \Delta_c \Delta_d}$ is short-hand for the product

$$\sqrt{\frac{\Delta_a \Delta_b}{\Delta_j}} \sqrt{\frac{\Delta_c \Delta_d}{\Delta_j}} \Delta_j$$

$$= (-1)^{(a+b-j)/2} (-1)^{(c+d-j)/2} (-1)^j \sqrt{\frac{[a+1][b+1]}{[j+1]}} \sqrt{\frac{[c+1][d+1]}{[j+1]}} [j+1]$$

$$= (-1)^{(a+b+c+d)/2} \sqrt{[a+1][b+1][c+1][d+1]}$$

In this form, since (a, b, j) and (c, d, j) are admissible triples, we see that this coeffient can be taken to be real, and its value is independent of the choice of i and j. The matrix $M[a, b, c, d]$ is real-valued.

It follows from Figure **??** (turn the diagrams by ninety degrees) that

$$M[a, b, c, d]^{-1} = M[b, d, a, c].$$

In Figure 42 we illustrate the formula

$$M[a, b, c, d]^T = M[b, d, a, c].$$

It follows from this formula that

$$M[a, b, c, d]^T = M[a, b, c, d]^{-1}.$$

Hence $M[a, b, c, d]$ is an orthogonal, real-valued matrix.

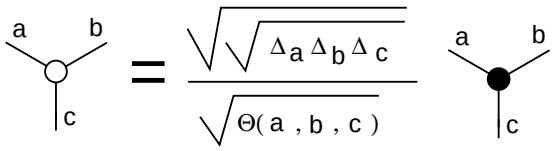

Figure 37: **Modified Three Vertex**

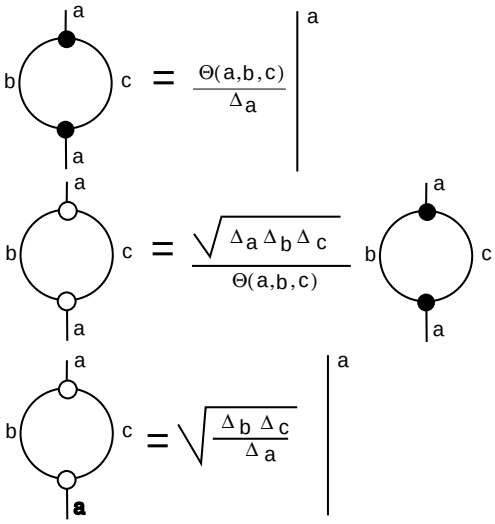

Figure 38: **Modified Bubble Identity**

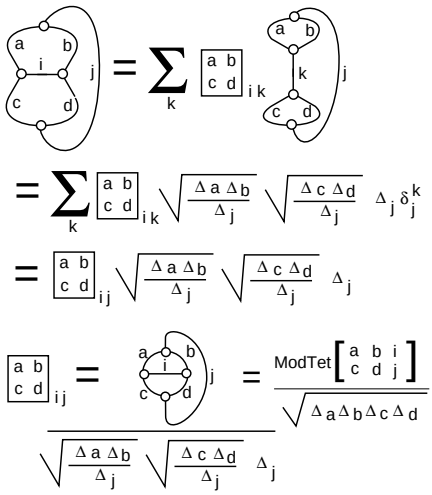

Figure 39: **Derivation of Modified Recoupling Coefficients**

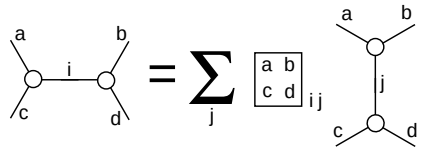

Figure 40: **Modified Recoupling Formula**

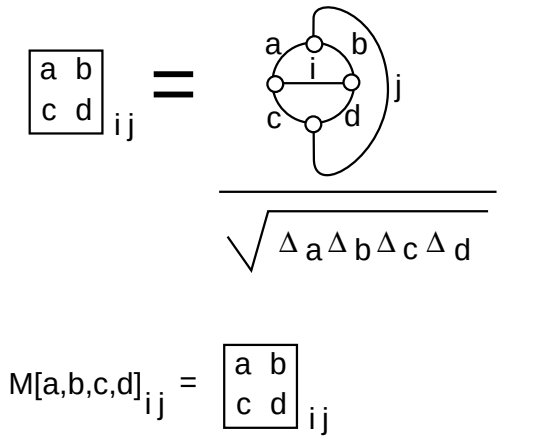

Figure 41: **Modified Recoupling Matrix**

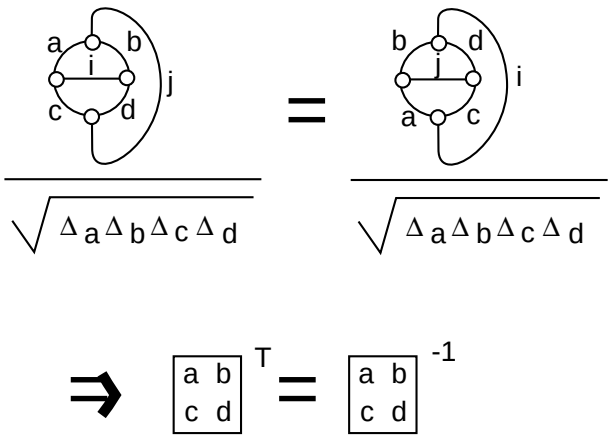

Figure 42: **Modified Matrix Transpose**

Theorem. In the Temperley-Lieb theory we obtain unitary (in fact real orthogonal) recoupling transformations when the bracket variable A has the form $A = e^{i\pi/2r}$ for r a positive integer. Thus we obtain families of unitary representations of the Artin braid group from the recoupling theory at these roots of unity.

Proof. The proof is given the discussion above. //

In Section 11 we shall show explictly how these methods work in the case of the Fibonacci model where $A = e^{3i\pi/5}$.

10 Fibonacci Particles

In this section and the next we detail how the Fibonacci model for anyonic quantum computing [65, 78] can be constructed by using a version of the two-stranded bracket polynomial and a generalization of Penrose spin networks. This is a fragment of the Temperly-Lieb recoupling theory [34]. We already gave in the preceding sections a general discussion of the theory of spin networks and their relationship with quantum computing.

The Fibonacci model is a $TQFT$ that is based on a single "particle" with two states that we shall call the *marked state* and the *unmarked state*. The particle in the marked state can interact with itself either to produce a single particle in the marked state, or to produce a single particle in the unmarked state. The particle in the unmarked state has no influence in interactions (an unmarked state interacting with any state S yields that state S). One way to indicate these two interactions symbolically is to use a box,for the marked state and a blank space for the unmarked state. Then one has two modes of interaction of a box with itself:

1. Adjacency: 

   and

2. Nesting:  .

With this convention we take the adjacency interaction to yield a single box, and the nesting interaction to produce nothing:

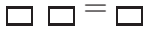

We take the notational opportunity to denote nothing by an asterisk (*). The syntatical rules for operating the asterisk are Thus the asterisk is a stand-in for no mark at all and it can be erased or placed wherever it is convenient to do so. Thus

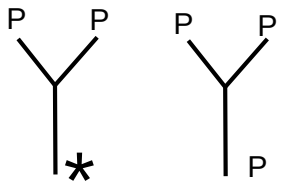

Figure 43: **Fibonacci Particle Interaction**

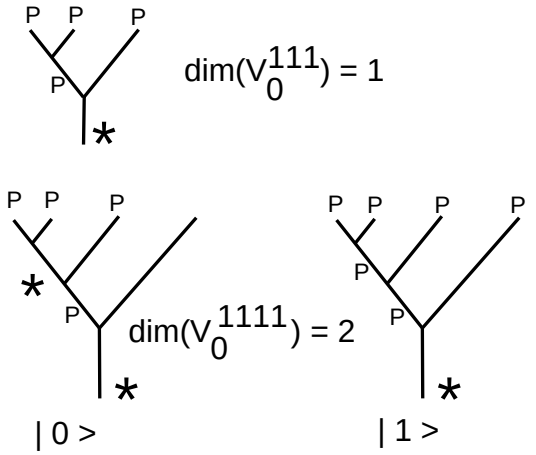

Figure 44: **Fibonacci Trees**

We shall make a recoupling theory based on this particle, but it is worth noting some of its purely combinatorial properties first. The arithmetic of combining boxes (standing for acts of distinction) according to these rules has been studied and formalized in [82] and correlated with Boolean algebra and classical logic. Here *within* and *next to* are ways to refer to the two sides delineated by the given distinction. From this point of view, there are two modes of relationship (adjacency and nesting) that arise at once in the presence of a distinction.

From here on we shall denote the Fibonaci particle by the letter P. Thus the two possible interactions of P with itself are as follows.

1. $P, P \longrightarrow *$
2. $P, P \longrightarrow P$

In Figure 44 we indicate in small tree diagrams the two possible interactions of the particle P with itself. In the first interaction the particle vanishes, producing the asterix. In the second interaction the particle a single copy of P is produced. These are the two basic actions of a single distinction relative to itself, and they constitute our formalism for this very elementary particle.

In Figure 44, we have indicated the different results of particle processes where we begin with a left-associated tree structure with three branches, all marked and then four branches all marked. In each case we demand that the particles interact successively to produce an unmarked particle in the end, at the root of the tree. More generally one can consider a left-associated tree with n upward branches and one root. Let $T(a_1, a_2, \cdots, a_n : b)$ denote such a tree with particle labels $a_1, \cdots, a_n$ on the top and root label b at the bottom of the tree. We consider all possible processes (sequences of particle interactions) that start with the labels at the top of the tree, and end with the labels at the bottom of the tree. Each such sequence is regarded as a basis vector in a complex vector space

$$V_b^{a_1, a_2, \cdots, a_n}$$

associated with the tree. In the case where all the labels are marked at the top and the bottom label is unmarked, we shall denote this tree by

$$V_0^{111\cdots 11} = V_0^{(n)}$$

where n denotes the number of upward branches in the tree. We see from Figure 44 that the dimension of $V_0^{(3)}$ is 1, and that

$$dim(V_0^{(4)}) = 2.$$

This means that $V_0^{(4)}$ is a natural candidate in this context for the two-qubit space.

Given the tree $T(1, 1, 1, \cdots, 1 : 0)$ (n marked states at the top, an unmarked state at the bottom), a process basis vector in $V_0^{(n)}$ is in direct correspondence with a string of boxes and asterisks (1's and 0's) of length $n - 2$ with no repeated asterisks and ending in a marked state. See Figure 44 for an illustration of the simplest cases. It follows from this that

$$dim(V_0^{(n)}) = f_{n-2}$$

where f_k denotes the k-th Fibonacci number:

$$f_0 = 1, f_1 = 1, f_2 = 2, f_3 = 3, f_4 = 5, f_5 = 8, \cdots$$

where

$$f_{n+2} = f_{n+1} + f_n.$$

The dimension formula for these spaces follows from the fact that there are f_n sequences of length $n - 1$ of marked and unmarked states with no repetition of an unmarked state. This fact is illustrated in Figure 45.

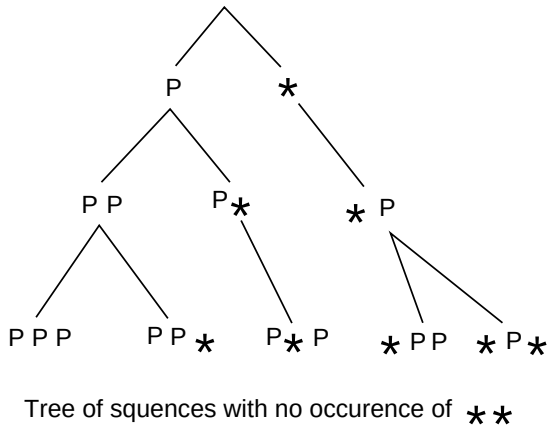

Figure 45: **Fibonacci Sequence**

11 The Fibonacci Recoupling Model

We now show how to make a model for recoupling the Fibonacci particle by using the Temperley Lieb recoupling theory and the bracket polynomial. Everything we do in this section will be based on the 2-projector, its properties and evaluations based on the bracket polynomial model for the Jones polynomial. While we have outlined the general recoupling theory based on the bracket polynomial in earlier sections of this paper, the present section is self-contained, using only basic information about the bracket polyonmial, and the essential properties of the 2-projector as shown in Figure 46. In this figure we state the definition of the 2-projector, list its two main properties (the operator is idempotent and a self-attached strand yields a zero evaluation) and give diagrammatic proofs of these properties.

In Figure 47, we show the essence of the Temperley-Lieb recoupling model for the Fibonacci particle. The Fibonacci particle is, in this mathematical model, identified with the 2-projector itself. As the reader can see from Figure 47, there are two basic interactions of the 2-projector with itself, one giving a 2-projector, the other giving nothing. This is the pattern of self-iteraction of the Fibonacci particle. There is a third possibility, depicted in Figure 47, where two 2-projectors interact to produce a 4-projector. We could remark at the outset, that the 4-projector will be zero if we choose the bracket polynomial variable $A = e^{i3\pi/5}$. Rather than start there, we will assume that the 4-projector is forbidden and deduce (below) that the theory has to be at this root of unity.

Note that in Figure 47 we have adopted a single strand notation for the particle interactions, with a solid strand corresponding to the marked particle, a dotted strand (or nothing) corresponding to the unmarked particle. A dark vertex indicates either an interaction point, or it may be used to indicate the single strand is shorthand for two ordinary strands. Remember that these are all shorthand expressions for underlying bracket polynomial calculations.

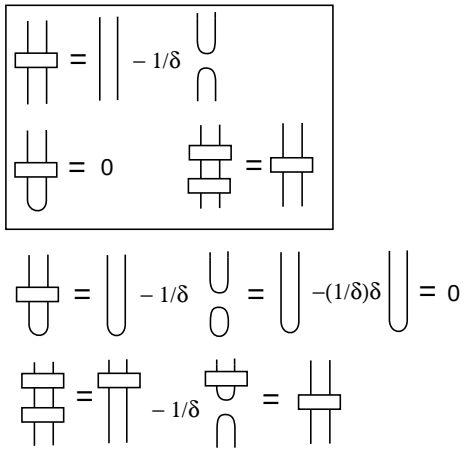

Figure 46: **The 2-Projector**

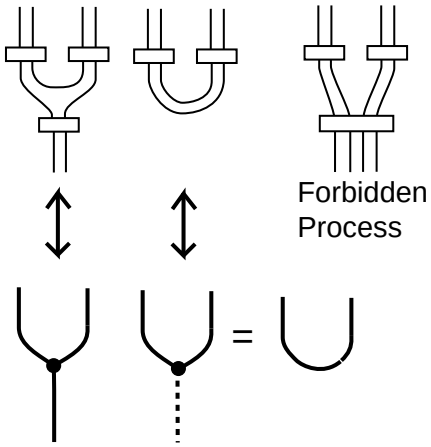

Figure 47: **Fibonacci Particle as 2-Projector**

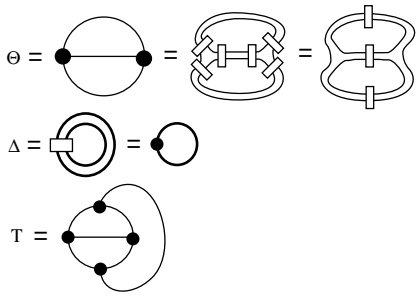

Figure 48: **Theta, Delta and Tetrahedron**

In Figure 48, Figure 49, Figure 50, Figure 51, Figure 52 and Figure 53 we have provided complete diagrammatic calculations of all of the relevant small nets and evaluations that are useful in the two-strand theory that is being used here. The reader may wish to skip directly to Figure 54 where we determine the form of the recoupling coefficients for this theory. We will discuss the resulting algebra below.

For the reader who does not want to skip the next collection of figures, here is a guided tour. Figure 48 illustrates three three basic nets in case of two strands. These are the theta, delta and tetrahedron nets. In this figure we have shown the decomposition on the theta and delta nets in terms of 2-projectors. The Tetrahedron net will be similarly decomposed in Figure 52 and Figure 53. The theta net is denoted Θ, the delta by Δ, and the tetrahedron by T. In Figure 49 we illustrate how a pedant loop has a zero evaluation. In Figure 50 we use the identity in Figure 49 to show how an interior loop (formed by two trivalent vertices) can be removed and replaced by a factor of Θ/Δ. Note how, in this figure, line two proves that one network is a multiple of the other, while line three determines the value of the multiple by closing both nets.

Figure 51 illustrates the explicit calculation of the delta and theta nets. The figure begins with a calculation of the result of closing a single strand of the 2-projector. The result is a single stand multiplied by $(\delta - 1/\delta)$ where $\delta = -A^2 - A^{-2}$, and A is the bracket polynomial parameter. We then find that

$$\Delta = \delta^2 - 1$$

and

$$\Theta = (\delta - 1/\delta)^2\delta - \Delta/\delta = (\delta - 1/\delta)(\delta^2 - 2).$$

Figure 52 and Figure 53 illustrate the calculation of the value of the tetrahedral network T. The reader should note the first line of Figure 52 where the tetradedral net is translated into a pattern of 2-projectors, and simplified. The rest of these two figures are a diagrammatic calculation, using the expansion formula for the 2-projector. At the end of Figure 53 we obtain the formula for the tetrahedron

$$T = (\delta - 1/\delta)^2(\delta^2 - 2) - 2\Theta/\delta.$$

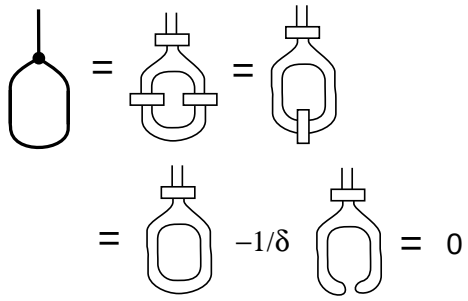

Figure 49: **LoopEvaluation–1**

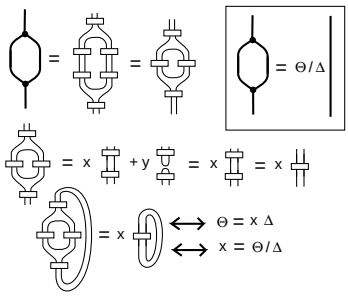

Figure 50: **LoopEvaluation–2**

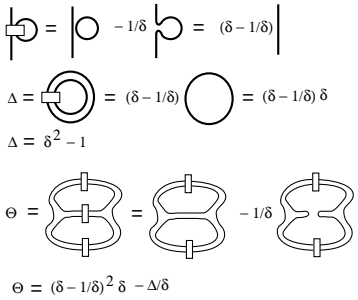

Figure 51: **Calculate Theta, Delta**

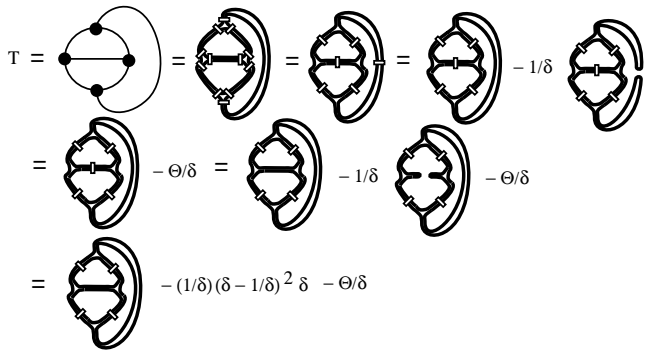

Figure 52: **Calculate Tetrahedron – 1**

Figure 54 is the key calculation for this model. In this figure we assume that the recoupling formulas involve only 0 and 2 strands, with 0 corresponding to the null particle and 2 corresponding to the 2-projector. ($2+2 = 4$ is forbidden as in Figure 47.) From this assumption we calculate that the recoupling matrix is given by

$$F = \begin{pmatrix} a & b \\ c & d \end{pmatrix} = \begin{pmatrix} 1/\Delta & \Delta/\Theta \\ \Theta/\Delta^2 & T\Delta/\Theta^2 \end{pmatrix}$$

Figure 55 and Figure 56 work out the exact formulas for the braiding at a three-vertex in this theory. When the 3-vertex has three marked lines, then the braiding operator is multiplication by $-A^4$, as in Figure 55 . When the 3-vertex has two marked lines, then the braiding operator is multiplication by A^8, as shown in Figure 56.

Notice that it follows from the symmetry of the diagrammatic recoupling formulas of Figure 54 that *the square of the recoupling matrix F is equal to the identity.* That is,

$$\begin{pmatrix} 1 & 0 \\ 0 & 1 \end{pmatrix} = F^2 = \begin{pmatrix} 1/\Delta & \Delta/\Theta \\ \Theta/\Delta^2 & T\Delta/\Theta^2 \end{pmatrix} \begin{pmatrix} 1/\Delta & \Delta/\Theta \\ \Theta/\Delta^2 & T\Delta/\Theta^2 \end{pmatrix} =$$

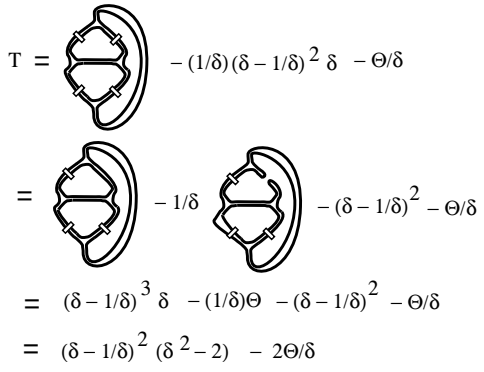

Figure 53: **Calculate Tetrahedron – 2**

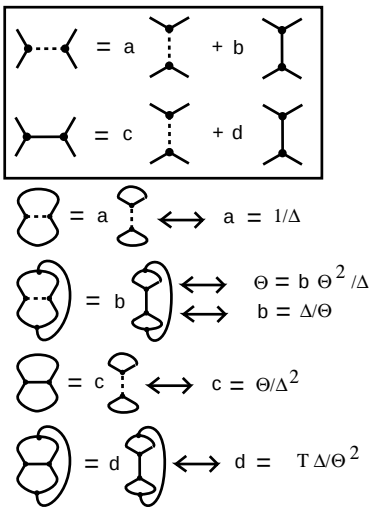

Figure 54: **Recoupling for 2-Projectors**

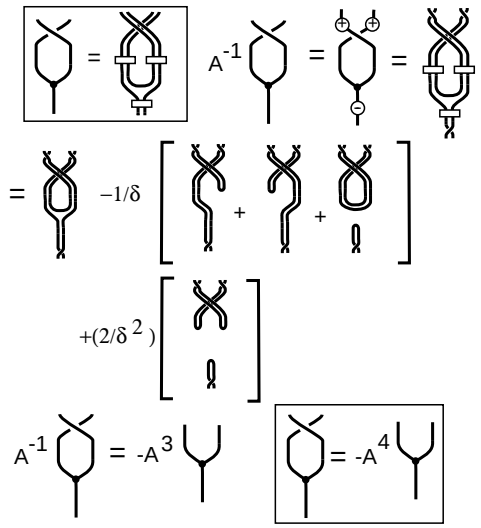

Figure 55: **Braiding at the Three-Vertex**

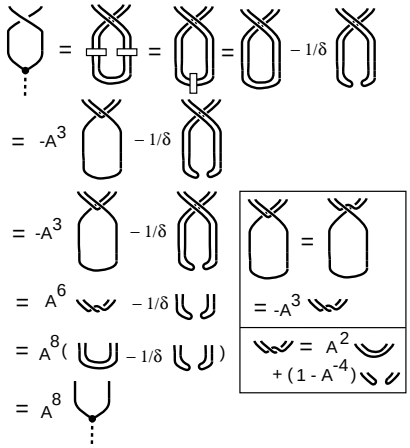

Figure 56: **Braiding at the Null-Three-Vertex**

$$\begin{pmatrix} 1/\Delta^2 + 1/\Delta & 1/\Theta + T\Delta^2/\Theta^3 \\ \Theta/\Delta^3 + T/(\Delta\Theta) & 1/\Delta + \Delta^2 T^2/\Theta^4 \end{pmatrix}.$$

Thus we need the relation

$$1/\Delta + 1/\Delta^2 = 1.$$

This is equivalent to saying that

$$\Delta^2 = 1 + \Delta,$$

a quadratic equation whose solutions are

$$\Delta = (1 \pm \sqrt{5})/2.$$

Furthermore, we know that

$$\Delta = \delta^2 - 1$$

from Figure 51. Hence

$$\Delta^2 = \Delta + 1 = \delta^2.$$

We shall now specialize to the case where

$$\Delta = \delta = (1 + \sqrt{5})/2,$$

leaving the other cases for the exploration of the reader. We then take

$$A = e^{3\pi i/5}$$

so that

$$\delta = -A^2 - A^{-2} = -2cos(6\pi/5) = (1 + \sqrt{5})/2.$$

Note that $\delta - 1/\delta = 1$. Thus

$$\Theta = (\delta - 1/\delta)^2\delta - \Delta/\delta = \delta - 1.$$

and

$$T = (\delta - 1/\delta)^2(\delta^2 - 2) - 2\Theta/\delta = (\delta^2 - 2) - 2(\delta - 1)/\delta$$
$$= (\delta - 1)(\delta - 2)/\delta = 3\delta - 5.$$

Note that

$$T = -\Theta^2/\Delta^2,$$

from which it follows immediately that

$$F^2 = I.$$

This proves that we can satisfy this model when $\Delta = \delta = (1 + \sqrt{5})/2$.

For this specialization we see that the matrix F becomes

$$F = \begin{pmatrix} 1/\Delta & \Delta/\Theta \\ \Theta/\Delta^2 & T\Delta/\Theta^2 \end{pmatrix} = \begin{pmatrix} 1/\Delta & \Delta/\Theta \\ \Theta/\Delta^2 & (-\Theta^2/\Delta^2)\Delta/\Theta^2 \end{pmatrix} = \begin{pmatrix} 1/\Delta & \Delta/\Theta \\ \Theta/\Delta^2 & -1/\Delta \end{pmatrix}$$

This version of F has square equal to the identity independent of the value of Θ, so long as $\Delta^2 = \Delta + 1$.

The Final Adjustment. Our last version of F suffers from a lack of symmetry. It is not a symmetric matrix, and hence not unitary. A final adjustment of the model gives this desired symmetry. *Consider the result of replacing each trivalent vertex (with three 2-projector strands) by a multiple by a given quantity* α. Since the Θ has two vertices, it will be multiplied by α^2. Similarly, the tetradhedron T will be multiplied by α^4. The Δ and the δ will be unchanged. Other properties of the model will remain unchanged. The new recoupling matrix, after such an adjustment is made, becomes

$$\begin{pmatrix} 1/\Delta & \Delta/\alpha^2\Theta \\ \alpha^2\Theta/\Delta^2 & -1/\Delta \end{pmatrix}$$

For symmetry we require

$$\Delta/(\alpha^2\Theta) = \alpha^2\Theta/\Delta^2.$$

We take

$$\alpha^2 = \sqrt{\Delta^3}/\Theta.$$

With this choice of α we have

$$\Delta/(\alpha^2\Theta) = \Delta\Theta/(\Theta\sqrt{\Delta^3}) = 1/\sqrt{\Delta}.$$

Hence the new symmetric F is given by the equation

$$F = \begin{pmatrix} 1/\Delta & 1/\sqrt{\Delta} \\ 1/\sqrt{\Delta} & -1/\Delta \end{pmatrix} = \begin{pmatrix} \tau & \sqrt{\tau} \\ \sqrt{\tau} & -\tau \end{pmatrix}$$

where Δ is the golden ratio and $\tau = 1/\Delta$. This gives the Fibonacci model. Using Figure 55 and Figure 56, we have that the local braiding matrix for the model is given by the formula below with $A = e^{3\pi i/5}$.

$$R = \begin{pmatrix} -A^4 & 0 \\ 0 & A^8 \end{pmatrix} = \begin{pmatrix} e^{4\pi i/5} & 0 \\ 0 & -e^{2\pi i/5} \end{pmatrix}.$$

The simplest example of a braid group representation arising from this theory is the representation of the three strand braid group generated by $S_1 = R$ and $S_2 = FRF$ (Remember that $F = F^T = F^{-1}$.). The matrices S_1 and S_2 are both unitary, and they generate a dense subset of the unitary group $SU(2)$, supplying the first part of the transformations needed for quantum computing.

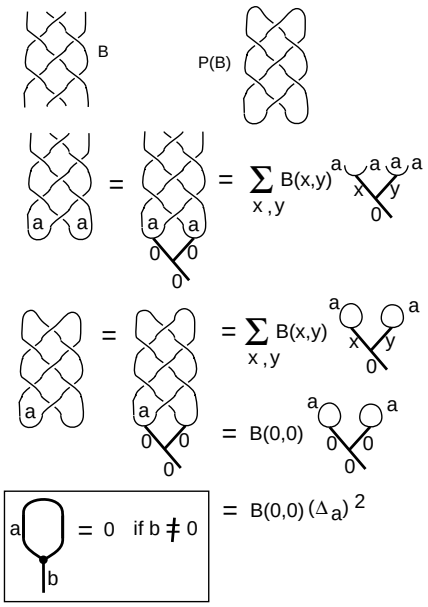

Figure 57: **Evaluation of the Plat Closure of a Braid**

12 Quantum Computation of Colored Jones Polynomials and the Witten-Reshetikhin-Turaev Invariant

In this section we make some brief comments on the quantum computation of colored Jones polynomials. This material will be expanded in a subsequent publication.

First, consider Figure 57. In that figure we illustrate the calculation of the evalutation of the *(a) - colored bracket polynomial* for the *plat closure* $P(B)$ of a braid B. The reader can infer the definition of the plat closure from Figure 57. One takes a braid on an even number of strands and closes the top strands with each other in a row of maxima. Similarly, the bottom strands are closed with a row of minima. It is not hard to see that any knot or link can be represented as the plat closure of some braid. Note that in this figure we indicate the action of the braid group on the process spaces corresponding to the small trees attached below the braids.

The (a) - colored bracket polynonmial of a link L, denoted $< L >_a$, is the evaluation of that link where each single strand has been replaced by a parallel strands and the insertion of Jones-Wenzl projector (as discussed in Section 9). We then see that we can use our discussion of the Temperley-Lieb recoupling theory as in sections 7,8 and 9 to compute the value of the colored bracket polynomial for the plat closure PB. As shown in Figure 57, we regard the braid as acting on a process space $V_0^{a,a,\cdots,a}$ and take the case of the action on the vector v whose process space coordinates are all zero. Then the action of the braid takes the form

$$Bv(0,\cdots,0) = \Sigma_{x_1,\cdots,x_n} B(x_1,\cdots,x_n) v(x_1,\cdots,x_n)$$

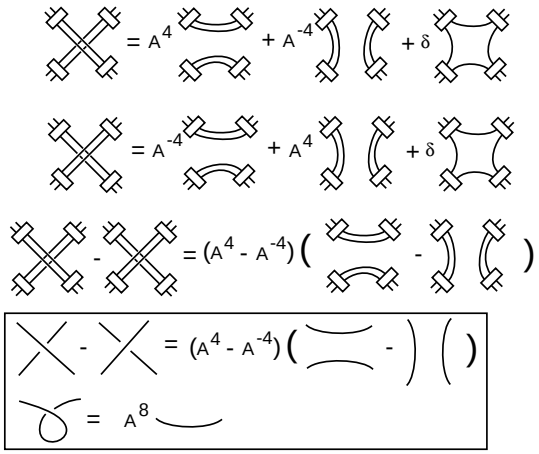

Figure 58: **Dubrovnik Polynomial Specialization at Two Strands**

where $B(x_1, \cdots, x_n)$ denotes the matrix entries for this recoupling transformation and $v(x_1, \cdots, x_n)$ runs over a basis for the space $V_0^{a,a,\cdots,a}$. Here n is even and equal to the number of braid strands. In the figure we illustrate with $n = 4$. Then, as the figure shows, when we close the top of the braid action to form PB, we cut the sum down to the evaluation of just one term. In the general case we will get

$$< PB >_a = B(0, \cdots, 0)\Delta_a^{n/2}.$$

The calculation simplifies to this degree because of the vanishing of loops in the recoupling graphs. The vanishing result is stated in Figure 57, and it is proved in the case $a = 2$ in Figure 49.

The *colored Jones polynomials* are normalized versions of the colored bracket polymomials, differing just by a normalization factor.

In order to consider quantum computation of the colored bracket or colored Jones polynomials, we therefore can consider quantum computation of the matrix entries $B(0, \cdots, 0)$. These matrix entries in the case of the roots of unity $A = e^{i\pi/2r}$ and for the $a = 2$ Fibonacci model with $A = e^{3i\pi/5}$ are parts of the diagonal entries of the unitary transformation that represents the braid group on the process space $V_0^{a,a,\cdots,a}$. *We can obtain these matrix entries by using the Hadamard test as described in section 6.* As a result we get relatively efficient quantum algorithms for the colored Jones polynonmials at these roots of unity, in essentially the same framework as we described in section 6, but for braids of arbitrary size. The computational complexity of these models is essentially the same as the models for the Jones polynomial discussed in [1]. We reserve discussion of these issues to a subsequent publication.

It is worth remarking here that these algorithms give not only quantum algorithms for computing the colored bracket and Jones polynomials, but also for computing the Witten-Reshetikhin-Turaev (WRT) invariants at the above roots of unity. The reason for this is that the WRT

invariant, in unnormalized form is given as a finite sum of colored bracket polynomials:

$$WRT(L) = \Sigma_{a=0}^{r-2} \Delta_a < L >_a,$$

and so the same computation as shown in Figure 57 applies to the WRT. This means that we have, in principle, a quantum algorithm for the computation of the Witten functional integral [86] via this knot-theoretic combinatorial topology. It would be very interesting to understand a more direct approach to such a computation via quantum field theory and functional integration.

Finally, we note that in the case of the Fibonacci model, the (2)-colored bracket polynomial is a special case of the Dubrovnik version of the Kauffman polynomial [36]. See Figure 58 for diagammatics that resolve this fact. The skein relation for the Dubrovnik polynomial is boxed in this figure. Above the box, we show how the double strands with projectors reproduce this relation. This observation means that in the Fibonacci model, the natural underlying knot polynomial is a special evaluation of the Dubrovnik polynomial, and the Fibonacci model can be used to perform quantum computation for the values of this invariant.

13 A Direct Construction of the Fibonacci Model

In section 5 of this paper, we give elementary constructions for unitary representations of the three strand braid group in $U(2)$. In section 6 we show how to use unitary representations of the three strand brand group to devise a quantum computation for the Jones polynomial. In this section we return to these considerations, and show how to construct the Fibonacci model by elementary means, without using the recoupling theory that we have explained in the previous sections of the paper. This final approach is significant in that it shows an even closer relationship of the Fibonacci model with the Temperley Lieb algebra representation associated with the Jones polynomial.

The constructions in this section are based on the combinatorics of the Fibonacci model. While we do not assume the recoupling theory of the previous sections, we essentially reconstruct its patterns for the particular purposes of the Fibonacci model. Recall that in the Fibonacci model we have a (mathematical) particle P that interacts with itself either to produce P or to produce a neutral particle $*$. If X is any particle then $*$ interacts with X to produce X. Thus $*$ acts as an identity trasformation. These rules of interaction are illustrated in Figure 43, Figure 44, Figure 45 and Figure 59.

The braiding of two particles is measured in relation to their interaction. In Figure 60 we illustrate braiding of P with itself in relation to the two possible interactions of P with itself. If P interacts to produce $*$, then the braiding gives a phase factor of μ. If P interacts to produce P, then the braiding gives a phase factor of λ. We assume at the outset that μ and λ are unit complex numbers. One should visualize these particles as moving in a plane and the diagrams of interaction are either creations of two particles from one particle, or fusions of two particles to a

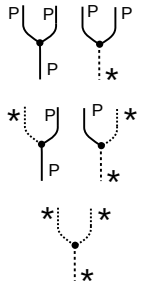

Figure 59: **The Fibonacci Particle** P

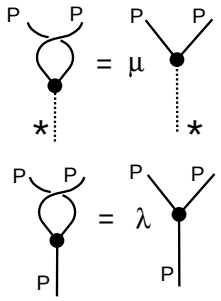

Figure 60: **Local Braiding**

single particle (depending on the choice of temporal direction). Thus we have a braiding matrix for these "local" particle interactions:

$$R = \begin{pmatrix} \mu & 0 \\ 0 & \lambda \end{pmatrix}$$

written with respect to the basis $\{|*\rangle, |P\rangle\}$ for this space of particle interactions.

We want to make this braiding matrix part of a larger representation of the braid group. In particular, we want a representation of the three-strand braid group on the process space V_3 illustrated in Figure 3. This space starts with three P particles and considers processes associated in the patttern $(PP)P$ with the stipulation that the end product is P. The possible pathways are illustrated in Figure 61. They correspond to $(PP)P \longrightarrow (*)P \longrightarrow P$ and $(PP)P \longrightarrow (P)P \longrightarrow P$. This process space has dimension two and can support a second braiding generator for the second two strands on the top of the tree. In order to articulate the second braiding we change basis to the process space corresponding to $P(PP)$ as shown in Figure 62 and Figure 63. The change of basis is shown in Figure 63 and has matrix F as shown below. We want a unitary representation ρ of three-strand braids so that $\rho(\sigma_1) = R$ and $\rho(\sigma_2) = S = F^{-1}RF$. See Figure 63. We take the form of the matrix F as follows.

$$F = \begin{pmatrix} a & b \\ b & -a \end{pmatrix}$$

where $a^2 + b^2 = 1$ with a and b real. This form of the matrix for the basis change is determined by the requirement that F is symmetric with $F^2 = I$. The symmetry of the change of basis formula essentially demands that $F^2 = I$. If F is real, symmetric and $F^2 = I$, then F is unitary. Since R is unitary we see that $S = FRF$ is also unitary. Thus, if F is constructed in this way then we obtain a unitary representation of B_3.

Now we try to simultaneously construct an F *and* construct a representation of the Temperley-Lieb algebra. We begin by noting that

$$R = \begin{pmatrix} \mu & 0 \\ 0 & \lambda \end{pmatrix} = \begin{pmatrix} \lambda & 0 \\ 0 & \lambda \end{pmatrix} + \begin{pmatrix} \mu - \lambda & 0 \\ 0 & 0 \end{pmatrix} = \begin{pmatrix} \lambda & 0 \\ 0 & \lambda \end{pmatrix} + \lambda^{-1} \begin{pmatrix} \delta & 0 \\ 0 & 0 \end{pmatrix}$$

where $\delta = \lambda(\mu - \lambda)$. Thus $R = \lambda I + \lambda^{-1}U$ where $U = \begin{pmatrix} \delta & 0 \\ 0 & 0 \end{pmatrix}$ so that $U^2 = \delta U$. For the Temperley-Lieb representation, we want $\delta = -\lambda^2 - \lambda^{-2}$. Hence we need $-\lambda^2 - \lambda^{-2} = \lambda(\mu - \lambda)$, which implies that $\mu = -\lambda^{-3}$. With this restriction on μ, we have the Temperley-Lieb representation and the corresponding unitary braid group representation for 2-strand braids and the 2-strand Temperley-Lieb algebra.

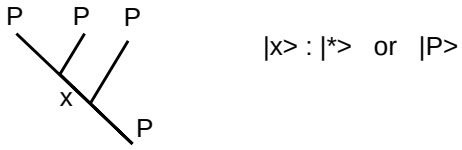

Figure 61: **Three Strands at Dimension Two**

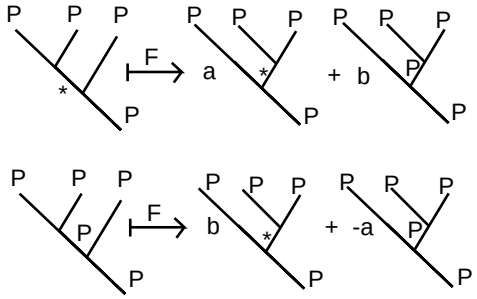

Figure 62: **Recoupling Formula**

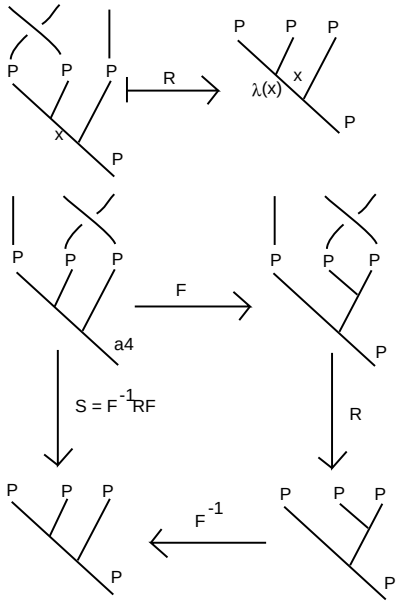

Figure 63: **Change of Basis**

Now we can go on to B_3 and TL_3 via $S = FRF = \lambda I + \lambda^{-1}V$ with $V = FUF$. We must examine V^2, UVU and VUV. We find that

$$V^2 = FUFFUF = FU^2F = \delta FUF = \delta V,$$

as desired and

$$V = FUF = \begin{pmatrix} a & b \\ b & -a \end{pmatrix} \begin{pmatrix} \delta & 0 \\ 0 & 0 \end{pmatrix} \begin{pmatrix} a & b \\ b & -a \end{pmatrix} = \delta \begin{pmatrix} a^2 & ab \\ ab & b^2 \end{pmatrix}.$$

Thus $V^2 = V$ and since $V = \delta|v\rangle\langle v|$ and $U = \delta|w\rangle\langle w|$ with $w = (1,0)^T$ and $v = Fw = (a,b)^T$ (T denotes transpose), we see that

$$VUV = \delta^3|v\rangle\langle v|w\rangle\langle w|v\rangle\langle v| = \delta^3 a^2|v\rangle\langle v| = \delta^2 a^2 V.$$

Similarly $UVU = \delta^2 a^2 U$. Thus, we need $\delta^2 a^2 = 1$ and so we shall take $a = \delta^{-1}$. With this choice, we have a representation of the Temperley-Lieb algebra TL_3 so that $\sigma_1 = AI + A^{-1}U$ and $\sigma_2 = AI + A^{-1}V$ gives a unitary representation of the braid group when $A = \lambda = e^{i\theta}$ and $b = \sqrt{1 - \delta^{-2}}$ is real. This last reality condition is equivalent to the inequality

$$cos^2(2\theta) \geq \frac{1}{4},$$

which is satisfied for infinitely many values of θ in the ranges

$$[0, \pi/6] \cup [\pi/3, 2\pi/3] \cup [5\pi/6, 7\pi/6] \cup [4\pi/3, 5\pi/3].$$

With these choices we have

$$F = \begin{pmatrix} a & b \\ b & -a \end{pmatrix} = \begin{pmatrix} 1/\delta & \sqrt{1-\delta^{-2}} \\ \sqrt{1-\delta^{-2}} & -1/\delta \end{pmatrix}$$

real and unitary, and for the Temperley-Lieb algebra,

$$U = \begin{pmatrix} \delta & 0 \\ 0 & 0 \end{pmatrix}, V = \delta \begin{pmatrix} a^2 & ab \\ ab & b^2 \end{pmatrix} = \begin{pmatrix} a & b \\ b & \delta b^2 \end{pmatrix}.$$

Now examine Figure 64. Here we illustrate the action of the braiding and the Temperley-Lieb Algebra on the first Fibonacci process space with basis $\{|*\rangle, |P\rangle\}$. Here we have $\sigma_1 = R, \sigma_2 = FRF$ and $U_1 = U, U_2 = V$ as described above. Thus we have a representation of the braid group on three strands and a representation of the Temperley-Lieb algebra on three strands with no further restrictions on δ.

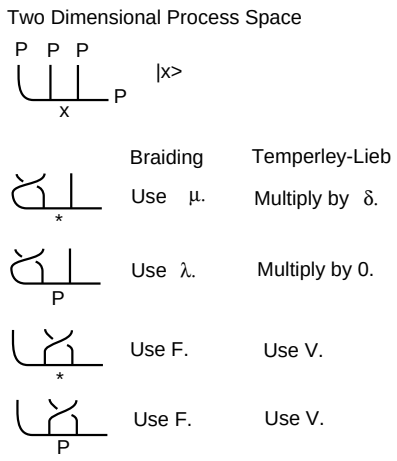

Figure 64: **Algebra for a Two Dimensional Process Space**

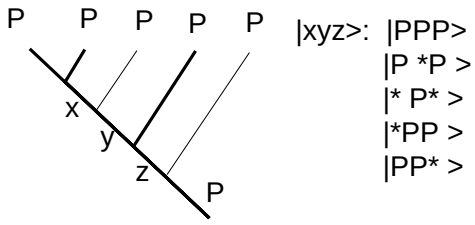

Figure 65: **A Five Dimensional Process Space**

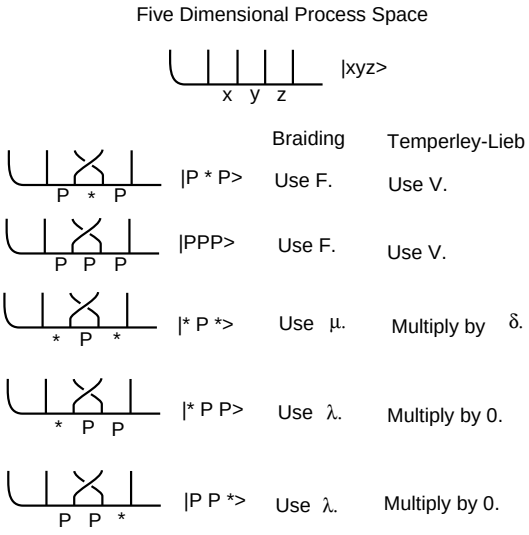

Figure 66: **Algebra for a Five Dimensional Process Space**

So far, we have arrived at exactly the 3-strand braid representations that we used in our papers [58, 60] giving a quantum algorithm for the Jones polynomial for three-strand braids. In this paper we are working in the context of the Fibonacci process spaces and so we wish to see how to make a representation of the Temperley-Lieb algebra to this model as a whole, not restricting ourselves to only three strands. The generic case to consider is the action of the Temperley-Lieb algebra on process spaces of higher dimension as shown in Figure 65 and Figure 66. In Figure 66 we have illustrated the triplets from the previous figure as part of a possibly larger tree and have drawn the strings horizontally rather than diagonally. In this figure we have listed the effects of braiding the vertical strands 3 and 4. We see from this figure that the action of the Temperley-Lieb algebra must be as follows:

$$U_3|P*P\rangle = a|P*P\rangle + b|PPP\rangle,$$
$$U_3|PPP\rangle = b|P*P\rangle + \delta b^2|PPP\rangle,$$
$$U_3|*P*\rangle = \delta|*P*\rangle,$$
$$U_3|*PP\rangle = 0,$$
$$U_3|PP*\rangle = 0.$$

Here we have denoted this action as U_3 because it connotes the action on the third and fourth vertical strands in the sequences shown in Figure 66. Note that in a larger sequence we can recognize U_j by examining the triplet surrounding the $j-1$-th element in the sequence, just as the pattern above is governed by the elements surrounding the second element in the sequence. For simplicity, we have only indicated three elements in the sequences above. Note that in a sequence for the Fibonacci process there are never two consecutive appearances of the neutral element $*$.

We shall refer to a sequence of $*$ and P as a *Fibonacci sequence* if it contains no consecutive appearances of $*$. Thus $|PP*P*P*P\rangle$ is a Fibonacci sequence. In working with this representation of the braid group and Temperley-Lieb algebra, it is convenient to assume that the ends of the sequence are flanked by P as in Figure 65 and Figure 66 for sequences of length 3. It is convenient to leave out the flanking P's when notating the sequence.

Using these formulas we can determine conditions on δ such that this is a representation of the Temperley-Lieb algebra for all Fibonacci sequences. Consider the following calculation:

$$U_4U_3U_4|PPPP\rangle = U_3U_2(b|PP*P\rangle + \delta b^2|PPPP\rangle)$$
$$= U_4(bU_3|PP*P\rangle + \delta b^2U_3|PPPP\rangle)$$
$$= U_4(0 + \delta b^2(b|P*PP\rangle + \delta b^2|PPPP\rangle)$$
$$= \delta b^2(bU_4|P*PP\rangle + \delta b^2U_4|PPPP\rangle)$$
$$= \delta^2b^4U_4|PPPP\rangle.$$

Thus we see that in order for $U_4U_3U_4 = U_4$, we need that $\delta^2b^4 = 1$.

It is easy to see that $\delta^2 b^4 = 1$ is the only remaining condition needed to make sure that the action of the Temperley-Lieb algebra extends to all Fibonacci Model sequences.

Note that $\delta^2 b^4 = \delta^2(1-\delta^{-2})^2 = (\delta - 1/\delta)^2$. Thus we require that

$$\delta - 1/\delta = \pm 1.$$

When $\delta - 1/\delta = 1$, we have the solutions $\delta = \frac{1\pm\sqrt{5}}{2}$. However, for the reality of F we require that $1 - \delta^{-2} \geq 0$, ruling out the choice $\delta = \frac{1-\sqrt{5}}{2}$. When $\delta - 1/\delta = -1$, we have the solutions $\delta = \frac{-1\pm\sqrt{5}}{2}$. This leaves only $\delta = \pm\phi$ where $\phi = \frac{1+\sqrt{5}}{2}$ (the Golden Ratio) as possible values for δ that satisfy the reality condition for F. Thus, up to a sign we have arrived at the well-known value of $\delta = \phi$ (the Fibonacci model) as essentially the only way to have an extension of this form of the representation of the Temperley-Lieb algebra for n strands. Let's state this positively as a Theorem.

Fibonacci Theorem. Let V_{n+2} be the complex vector space with basis $\{|x_1 x_2 \cdots x_n\rangle\}$ where each x_i equals either P or $*$ and there do *not* occur two consecutive appearances of $*$ in the sequence $\{x_1, \cdots x_n\}$. We refer to this basis for V_n as the set of *Fibonacci sequences* of length n. Then the dimension of V_n is equal to f_{n+1} where f_n is the n-th Fibonacci number: $f_0 = f_1 = 1$ and $f_{n+1} = f_n + f_{n-1}$. Let $\delta = \pm\phi$ where $\phi = \frac{1+\sqrt{5}}{2}$. Let $a = 1/\delta$ and $b = \sqrt{1-a^2}$. Then the Temperley-Lieb algebra on $n+2$ strands with loop value δ acts on V_n via the formulas given below. First we give the left-end actions.

$$U_1|*x_2x_3\cdots x_n\rangle = \delta|*x_2x_3\cdots x_n\rangle,$$
$$U_1|Px_2x_3\cdots x_n\rangle = 0,$$
$$U_2|*Px_3\cdots x_n\rangle = a|*Px_3\cdots x_n\rangle + b|PPx_3\cdots x_n\rangle,$$
$$U_2|P*x_3\cdots x_n\rangle = 0,$$
$$U_2|PPx_3\cdots x_n\rangle = b|*Px_3\cdots x_n\rangle + \delta b^2|PPx_3\cdots x_n\rangle.$$

Then we give the general action for the middle strands.

$$U_i|x_1\cdots x_{i-3}P*Px_{i+1}\cdots x_n\rangle = a|x_1\cdots x_{i-3}P*Px_{i+1}\cdots x_n\rangle$$
$$+b|x_1\cdots x_{i-3}PPPx_{i+1}\cdots x_n\rangle,$$
$$U_i|x_1\cdots x_{i-3}PPPx_{i+1}\cdots x_n\rangle = b|x_1\cdots x_{i-3}P*Px_{i+1}\cdots x_n\rangle$$
$$+\delta b^2|x_1\cdots x_{i-3}PPPx_{i+1}\cdots x_n\rangle,$$
$$U_i|x_1\cdots x_{i-3}*P*x_{i+1}\cdots x_n\rangle = \delta|x_1\cdots x_{i-3}*P*x_{i+1}\cdots x_n\rangle,$$
$$U_i|x_1\cdots x_{i-3}*PPx_{i+1}\cdots x_n\rangle = 0,$$
$$U_i|x_1\cdots x_{i-3}PP*x_{i+1}\cdots x_n\rangle = 0.$$

Finally, we give the right-end action.

$$U_{n+1}|x_1\cdots x_{n-2}*P\rangle = 0,$$
$$U_{n+1}|x_1\cdots x_{n-2}P*\rangle = 0,$$
$$U_{n+1}|x_1\cdots x_{n-2}PP\rangle = b|x_1\cdots x_{n-2}P*\rangle + \delta b^2|x_1\cdots x_{n-2}PP\rangle.$$

Remark. Note that the left and right end Temperley-Lieb actions depend on the same basic pattern as the middle action. The Fibonacci sequences $|x_1 x_2 \cdots x_n\rangle$ should be regarded as flanked left and right by P's just as in the special cases discussed prior to the proof of the Fibonacci Theorem.

Corollary. With the hypotheses of Theorem 2, we have a unitary representation of the Artin Braid group B_{n+2} to TL_{n+2}, $\rho : B_{n+2} \longrightarrow TL_{n+2}$ given by the formulas

$$\rho(\sigma_i) = AI + A^{-1}U_i,$$

$$\rho(\sigma_i^{-1}) = A^{-1}I + AU_i,$$

where $A = e^{3\pi i/5}$ where the U_i connote the representation of the Temperley-Lieb algebra on the space V_{n+2} of Fibonacci sequences as described in the Theorem above.

Remark. The Theorem and Corollary give the original parameters of the Fibonacci model and shows that this model admits a unitary representation of the braid group via a Jones representation of the Temperley-Lieb algebra.

In the original Fibonacci model [57], there is a basic non-trivial recoupling matrix F.

$$F = \begin{pmatrix} 1/\delta & 1/\sqrt{\delta} \\ 1/\sqrt{\delta} & -1/\delta \end{pmatrix} = \begin{pmatrix} \tau & \sqrt{\tau} \\ \sqrt{\tau} & -\tau \end{pmatrix}$$

where $\delta = \frac{1+\sqrt{5}}{2}$ is the golden ratio and $\tau = 1/\delta$. The local braiding matrix is given by the formula below with $A = e^{3\pi i/5}$.

$$R = \begin{pmatrix} A^8 & 0 \\ 0 & -A^4 \end{pmatrix} = \begin{pmatrix} e^{4\pi i/5} & 0 \\ 0 & -e^{2\pi i/5} \end{pmatrix}.$$

This is exactly what we get from our method by using $\delta = \frac{1+\sqrt{5}}{2}$ and $A = e^{3\pi i/5}$. Just as we have explained earlier in this paper, the simplest example of a braid group representation arising from this theory is the representation of the three strand braid group generated by $\sigma_1 = R$ and $\sigma_2 = FRF$ (Remember that $F = F^T = F^{-1}$.). The matrices σ_1 and σ_2 are both unitary, and they generate a dense subset of $SU(2)$, supplying the local unitary transformations needed for quantum computing. The full braid group representation on the Fibonacci sequences is computationally universal for quantum computation. In our earlier paper [57] and in the previous sections of the present work, we gave a construction for the Fibonacci model based on Temperely-Lieb recoupling theory. In this section, we have reconstructed the Fibonacci model on the more elementary grounds of the representation of the Temperley-Lieb algebra summarized in the statement of the Fibonacci Theorem and its Corollary.

References

[1] D. Aharonov, V. F. R. Jones, Z. Landau, A polynomial quantum algorithm for approximating the Jones polynomial. STOC'06: Proceedings of the 38th Annual ACM Symposium on Theory of Computing, 427436, ACM, New York, 2006. quant-ph/0511096.

[2] D. Aharonov, I. Arad, The BQP-hardness of approximating the Jones polynomial, quant-ph/0605181.

[3] J. Alicea and A. Stern, Designer non-Abelian anyon platforms: from Majorana to Fibonacci, Phys. Scr. T164 (2015) 014006 (10pp).

[4] P. K. Aravind, Borromean of the GHZ state. in 'Potentiality, Entanglement and Passion-at-a-Distance", ed. by R. S. Cohen et al, pp. 53-59, Kluwer, 1997.

[5] M.F. Atiyah, *The Geometry and Physics of Knots*, Cambridge University Press, 1990.

[6] R.J. Baxter. Exactly Solved Models in Statistical Mechanics. Acad. Press (1982).

[7] C. W. J. Beenakker, Search for Majorana Fermions in superconductors, arXiv: 1112.1950.

[8] G. Benkart, Commuting actions – a tale of two groups, in "Lie algebras and their representations (Seoul 1995)", Contemp. Math. Series, Vol. 194, American Mathematical Society (1996), pp. 1-46.

[9] J. Birman, Braids, Links, and Mapping Class Groups, Annals of Mathematics Series Number 82, (1974) Princeton University Press, Princeton, New Jersey.

[10] N. E. Bonesteel, L. Hormozi, G. Zikos and S. H. Simon, Braid topologies for quantum computation, Phys. Rev. Lett. 95 (2005), no. 14, 140503, 4 pp. quant-ph/0505665.

[11] S. H. Simon, N. E. Bonesteel, M. H. Freedman, N. Petrovic and L. Hormozi, Topological quantum computing with only one mobile quasiparticle, Phys. Rev. Lett. 96 (2006), no. 7, 070503, 4 pp., quant-ph/0509175.

[12] J. L. Brylinski and R. Brylinski, Universal quantum gates, in *Mathematics of Quantum Computation*, Chapman & Hall/CRC Press, Boca Raton, Florida, 2002 (edited by R. Brylinski and G. Chen).

[13] Chen, G., L. Kauffman, and S. Lomonaco, (eds.), "**Mathematics in Quantum Computation and Quantum Technology**," Chapman & Hall/CRC , (2007).

[14] L. Crane, 2-d physics and 3-d topology, *Comm. Math. Phys.* **135** (1991), no. 3, 615-640.

[15] B. Coecke, The logic of entanglement, quant-phy/0402014.

[16] S. Abramsky, B. Coecke, Categorical quantum mechanics. Handbook of quantum logic and quantum structuresquantum logic, 261323, Elsevier/North-Holland, Amsterdam, 2009.

[17] P.A.M. Dirac, *Principles of Quantum Mechanics*, Oxford University Press, 1958.

[18] H. A. Dye, Unitary solutions to the Yang-Baxter equation in dimension four. Quantum Inf. Process. 2 (2002), no. 1-2, 117151 (2003). arXiv:quant-ph/0211050.

[19] E. Fradkin and P. Fendley, Realizing non-abelian statistics in time-reversal invariant systems, Theory Seminar, Physics Department, UIUC, 4/25/2005.

[20] M. Freedman, A magnetic model with a possible Chern-Simons phase, With an appendix by F. Goodman and H. Wenzl. Comm. Math. Phys. 234 (2003), no. 1, 129183. quant-ph/0110060v1 9 Oct 2001, (2001).

[21] M. Freedman, *Topological Views on Computational Complexity*, Documenta Mathematica - Extra Volume ICM, 1998, pp. 453–464.

[22] M. Freedman, M. Larsen, and Z. Wang, A modular functor which is universal for quantum computation, Comm. Math. Phys. 227 (2002), no. 3, 605622. quant-ph/0001108v2, 1 Feb 2000.

[23] M. H. Freedman, A. Kitaev, Z. Wang, Simulation of topological field theories by quantum computers, *Commun. Math. Phys.*, **227**, 587-603 (2002), quant-ph/0001071.

[24] M. Freedman, Quantum computation and the localization of modular functors, Found. Comput. Math. 1 (2001), no. 2, 183204. quant-ph/0003128.

[25] C. Frohman and J. Kania-Bartoszynska, $SO(3)$ topological quantum field theory, *Comm. Anal. Geom.* **4**, (1996), no. 4, 589-679.

[26] D. A. Ivanov, Non-abelian statistics of half-quantum vortices in p-wave superconductors, Phys. Rev. Lett. 86, 268 (2001).

[27] F. Jaeger, D.L. Vertigan, D.J.A. Welsh, On the computational complexity of the Jones and Tutte polynomials, Math. Proc. Cam. Phil. Soc., Vol. 108, Issue 1, July 1990, pp. 35-53.

[28] V.F.R. Jones, A polynomial invariant for links via von Neumann algebras, Bull. Amer. Math. Soc. **129** (1985), 103–112.

[29] V.F.R.Jones. Hecke algebra representations of braid groups and link polynomials. Ann. of Math. 126 (1987), pp. 335-338.

[30] V.F.R.Jones. On knot invariants related to some statistical mechanics models. Pacific J. Math., vol. 137, no. 2 (1989), pp. 311-334.

[31] V. F. R. Jones, Braid groups, Hecke algebras and type II1 factors. "Geometric methods in operator algebras" (Kyoto, 1983), 242273, Pitman Res. Notes Math. Ser., 123, Longman Sci. Tech., Harlow, 1986.

[32] L.H. Kauffman, State models and the Jones polynomial, Topology **26** (1987), 395–407.

[33] L.H. Kauffman, Statistical mechanics and the Jones polynomial, AMS Contemp. Math. Series **78** (1989), 263–297.

[34] L.H. Kauffman, *Temperley-Lieb Recoupling Theory and Invariants of Three-Manifolds*, Princeton University Press, Annals Studies **114** (1994).

[35] L.H.Kauffman, New invariants in the theory of knots, *Amer. Math. Monthly*, Vol.95,No.3,March 1988. pp 195-242.

[36] L. H. Kauffman, An invariant of regular isotopy, *Trans. Amer. Math. Soc.* **318** (1990), no. 2, 417–471.

[37] L.H. Kauffman (ed.), *The Interface of Knots and Physics*, AMS PSAPM, Vol. 51, Providence, RI, 1996.

[38] L.H. Kauffman, *Knots and Physics*, World Scientific Publishers (1991), Second Edition (1993), Third Edition (2002), Fourth Edition (2012).

[39] L.H.Kauffman and D.E.Radford. Invariants of 3-manifolds derived from finite dimensional Hopf algebras. Journal of Knot Theory and its Ramifications, Vol.4, No.1 (1995), pp. 131-162.

[40] L. H. Kauffman, Functional Integration and the theory of knots, J. Math. Physics, Vol. 36 (5), May 1995, pp. 2402 - 2429.

[41] L. H. Kauffman and P. Noyes, Discrete physics and the Dirac equation, Physics Lett. A, No. 218 (1996), pp. 139-146.

[42] L.H. Kauffman and S. J. Lomonaco, Quantum entanglement and topological entanglement, New Journal of Physics **4** (2002), 73.1–73.18 (http://www.njp.org/).

[43] L. H. Kauffman, Teleportation Topology, quant-ph/0407224, (in the Proceedings of the 2004 Byelorus Conference on Quantum Optics), *Opt. Spectrosc.* 9, 2005, 227-232.

[44] L. H. Kauffman, math.GN/0410329, Knot diagrammatics. "Handbook of Knot Theory", edited by Menasco and Thistlethwaite, 233–318, Elsevier B. V., Amsterdam, 2005.

[45] L. H. Kauffman and T. Liko, hep-th/0505069, Knot theory and a physical state of quantum gravity, *Classical and Quantum Gravity*, Vol 23, ppR63 (2006).

[46] L.H. Kauffman and S. J. Lomonaco, Entanglement Criteria - Quantum and Topological, in *Quantum Information and Computation - Spie Proceedings, 21-22 April, 2003, Orlando, FL*, Donkor, Pinch and Brandt (eds.), Volume 5105, pp. 51–58.

[47] L. H. Kauffman and S. J. Lomonaco, Quantum knots, in *Quantum Information and Computation II, Proceedings of Spie, 12 -14 April 2004* (2004), ed. by Donkor Pirich and Brandt, pp. 268-284.

[48] S. J. Lomonaco and L. H. Kauffman, Quantum Knots and Mosaics, Journal of Quantum Information Processing, Vol. 7, Nos. 2-3, (2008), pp. 85 - 115. http://arxiv.org/abs/0805.0339

[49] S. J. Lomonaco and L. H. Kauffman, Quantum knots and lattices, or a blueprint for quantum systems that do rope tricks. Quantum information science and its contributions to mathematics, 209276, Proc. Sympos. Appl. Math., 68, Amer. Math. Soc., Providence, RI, 2010.

[50] S. J. Lomonaco and L. H. Kauffman, Quantizing braids and other mathematical structures: the general quantization procedure. In Brandt, Donkor, Pirich, editors, *Quantum Information and Comnputation IX - Spie Proceedings, April 2011*, Vol. 8057, of Proceedings of Spie, pp. 805702-1 to 805702-14, SPIE 2011.

[51] L. H. Kauffman and S. J. Lomonaco, Quantizing knots groups and graphs. In Brandt, Donkor, Pirich, editors, *Quantum Information and Comnputation IX - Spie Proceedings, April 2011*, Vol. 8057, of Proceedings of Spie, pp. 80570T-1 to 80570T-15, SPIE 2011.

[52] L. H. Kauffman and S. J. Lomonaco, Quantum Diagrams and Quantum Networks, SPIE Proc. on Quantum Information and Computation XII, Vol. 9173, (2014). pp. 91230P-1 to 91230P-14. http://arxiv.org/pdf/1404.4433.pdf

[53] S. J. Lomonaco and L. H. Kauffman, Quantizing Braids and Other Mathematical Objects: The General Quantization Procedure, SPIE Proc. on Quantum Information and Computation IX, Vol. 8057, (2011). pp. 805702-1 to 805702-14. http://arxiv.org/abs/1105.0371

[54] L. H. Kauffman and S. J. Lomonaco, Quantizing Knots and Beyond, SPIE Proc. on Quantum Information and Computation IX, Vol. 8057, (2011). pp. 805702-1 to 805702-14. http://arxiv.org/abs/1105.0152

[55] L. H. Kauffman and S. J. Lomonaco, Braiding Operators are Universal Quantum Gates, New Journal of Physics 6 (2004) 134, pp. 1-39.

[56] L. H. Kauffman and S. J. Lomonaco, q-deformed spin networks, knot polynomials and anyonic topological quantum computation. J. Knot Theory Ramifications 16 (2007), no. 3, 267–332.

[57] L. H. Kauffman and S. J. Lomonaco, Spin Networks and Quantum Computation, in "LIe Theory and Its Applications in Physics VII" eds. H. D. Doebner and V. K. Dobrev, Heron Press, Sofia (2008), pp. 225 - 239.

[58] L. H. Kauffman, Quantum computing and the Jones polynomial, math.QA/0105255, in *Quantum Computation and Information*, S. Lomonaco (ed.), AMS CONM/305, 2002, pp. 101–137.

[59] L. H. Kauffman and S. J. Lomonaco, Quantum Algorithms for the Jones Polynomial, SPIE Proc on Quantum Information and Computation VIII, Vol. 7702, (2010), 7702-03-1 to 7702-03-13. http://arxiv.org/pdf/1003.5426.pdf

[60] L. H. Kauffman and S. J. Lomonaco, Quantum entanglement and topological entanglement. New J. Phys. 4 (2002), 73.173.18.

[61] L. H. Kauffman and S. J. Lomonaco, The Fibonacci Model and the Temperley-Lieb Algebra. it International J. Modern Phys. B, Vol. 22, No. 29 (2008), 5065-5080.

[62] Rukhsan Ul Haq and L. H Kauffman, Z/2Z topological order and Majorana doubling in Kitaev Chain, (to appear) arXiv:1704.00252v1 [cond-mat.str-el].

[63] V. Mourik,K. Zuo, S. M. Frolov, S. R. Plissard, E.P.A.M. Bakkers, L.P. Kouwenhuven, Signatures of Majorana Fermions in hybred superconductor-semiconductor devices, arXiv: 1204.2792.

[64] A. Kitaev, Fault-tolerant quantum computation by anyons, Annals Phys. 303 (2003) 2-30. quant-ph/9707021.

[65] A. Kitaev, Anyons in an exactly solved model and beyond, Ann. Physics 321 (2006), no. 1, 2111. *arXiv.cond-mat/0506438 v1 17 June 2005*.

[66] T. Kohno, *Conformal Field Theory and Topology*, AMS Translations of Mathematical Monographs, Vol 210 (1998).

[67] S. J. Lomonaco (ed.), "Quantum Information Science and Its Contributons to Mathematics," AMS Proceedings of Applied Mathematics, Vol. 68, American Mathematics Society, Providence, RI, (2010).

[68] S. J. Lomonaco (ed.), "Quantum Computation: A Grand Mathematical Challenge for the Twenty-First Century and the Millennium," Proceedings of the Symposia of Appled Mathematics, vol. 58, American Mathematical Society, Providence, Rhode Island, (2002).

[69] S. J. Lomonaco and H. E. Brandt, (eds.), Quantum Computation and Information," AMS CONM, vol. 305, American Mathematical Society, Providence, RI, (2002).

[70] A. Marzuoli and M. Rasetti, Spin network quantum simulator, *Physics Letters A* **306** (2002) 79–87.

[71] S. Garnerone, A. Marzuoli, M. Rasetti, Quantum automata, braid group and link polynomials, quant-ph/0601169

[72] E. Majorana, A symmetric theory of electrons and positrons, I Nuovo Cimento,**14** (1937), pp. 171-184.

[73] S. A. Major, A spin network primer, arXiv:gr-qc/9905020.

[74] Li-Wei Yu and Mo-Lin Ge, More about the doubling degeneracy operators associated with Majorana Fermions and Yang-Baxter equation, Sci. Rep.**5**,8102(2015)

[75] G. Moore and N. Read, Noabelions in the fractional quantum Hall effect, *Nuclear Physics B360* (1991), 362 - 396.

[76] M. A. Nielsen and I. L. Chuang, " Quantum Computation and Quantum Information," Cambrige University Press, Cambridge (2000).

[77] R. Penrose, Angular momentum: An approach to Combinatorial Spacetime, In *Quantum Theory and Beyond*, edited by T. Bastin, Cambridge University Press (1969).

[78] J. Preskill, Topological computing for beginners, (slide presentation), Lecture Notes for Chapter 9 - Physics 219 - Quantum Computation. *http://www.iqi.caltech.edu/ preskill/ph219*

[79] N.Y. Reshetikhin and V. Turaev. Ribbon graphs and their invariants derived from quantum groups. Comm. Math. Phys. 127 (1990). pp. 1-26.

[80] N.Y. Reshetikhin and V. Turaev. Invariants of Three Manifolds via link polynomials and quantum groups. Invent. Math. 103, 547-597 (1991).

[81] J. Franko, E. C. Rowell, and Z. Wang, Extraspecial 2-Groups and Images of Braid Group Representations, Journal of Knot Theory and Its Ramifications Vol. 15, No. 4 (2006) 413427, World Scientific Publishing Company.

[82] G. Spencer–Brown, "Laws of Form," George Allen and Unwin Ltd. London (1969).

[83] V.G.Turaev. The Yang-Baxter equations and invariants of links. LOMI preprint E-3-87, Steklov Institute, Leningrad, USSR. Inventiones Math. 92 Fasc.3,527-553.

[84] V.G. Turaev and O. Viro. State sum invariants of 3-manifolds and quantum 6j symbols. Topology, Vol. 31, No. 4, pp. 865-902 (1992).

[85] F. Wilczek, *Fractional Statistics and Anyon Superconductivity,* World Scientific Publishing Company (1990).

[86] E. Witten, Quantum field Theory and the Jones Polynomial, *Commun. Math. Phys.*,vol. 121, 1989, pp. 351-399.

[87] P. Wocjan, J. Yard The Jones polynomial: quantum algorithms and applications in quantum complexity theory, quant-ph/0603069.

[88] C. N. Yang, Phys. Rev. Lett. **19** (1967) 1312.

[89] Y. Zhang, L.H. Kauffman and M. L. Ge, Yang-Baxterizations, universal quantum gates and Hamiltonians. *Quantum Inf. Process.* **4** (2005), no. 3, 159–197.